Pavol Jozef Šafárik University in Košice
Faculty of Science

Study of superconductivity in van der Waals heterostuctures of ferromagnet and superconductor

Košice 2021 Timon Moško

Pavol Jozef Šafárik University in Košice
Faculty of Science

Study of superconductivity in van der Waals heterostuctures of ferromagnet and superconductor

Bachelor thesis

Study program:	Physics
Department:	Institute of Physics
Supervisor:	RNDr. Martin Gmitra, PhD.

Košice 2021 Timon Moško

Univerzita P. J. Šafárika v Košiciach
Prírodovedecká fakulta

ZADANIE ZÁVEREČNEJ PRÁCE

Meno a priezvisko študenta: Timon Moško
Študijný program: Fyzika (Jednoodborové štúdium, bakalársky I. st., denná forma)
Študijný odbor: Fyzika
Typ záverečnej práce: Bakalárska práca
Jazyk záverečnej práce: slovenský
Sekundárny jazyk: anglický

Názov: Štúdium supravodivosti vo van der Waalsovských heteroštruktúrach feromagnetu a supravodiča

Názov EN: Study of superconductivity in van der Waals heterostuctures of ferromagnet-superconductor

Cieľ: Výpočet a analýza elektrónovej štruktúry modelového Hamiltoniánu efektívne popisujúceho supravodivosť vo van der Waalsovských heteroštruktúrach feromagnetu a supravodiča.

Literatúra:
[1] J. D. Sau et al., Phys. Rev. Lett. 104, 040502 (2010).
[2] M. Sato, S. Fujimoto, Phys. Rev. B 79, 094504 (2009).
[3] C. Nayak, S. H. Simon, A. Stern, M. Freedman, S. Das Sarma, Rev. Mod. Phys. 80, 1083 (2008).
[4] Jian-Xin Zhu, Bogoliubov-de Gennes: Method and Its Applications, Springer International Publishing Switzerland, 2016 ISBN 978-3-319-31312-2
[5] A. S. Alexandrov, Theory of Superconductivity: From Weak to Strong Coupling, Institute of Physics Publishing, Bristol and Philadelphia, 2003 ISBN 978-0750308366

Anotácia: Od objavenia grafénu ako prototypového dvojrozmerného materiálu, ktorý je semikovom, atomárne tenké materiály vykazujú takmer všetky materiálové vlastnosti aké poznáme, či už sú to kovy, polovodiče, izolátory, feromagnety, antiferomagnety alebo supravodiče. V súčasnej dobe jednou z najfascinujúcejších motivácií pri štúdiu atomárne tenkých dvojrozmerných materiálov je tzv. van der Waalsovská konštrukcia heteroštruktúr s dôrazom na vopred požadované vlastnosti systému. V tomto zmysle je možné vytvoriť úplne novu triedu materiálov s nepreskúmanými fyzikálnymi efektami. Uložením supravodiča k feromagnetu je možné generovať topologickú supravodivosť [1,2], ktorá je kľúčovou ingredienciou pre topologické kvantové počítanie [3]. V tejto bakalárskej práci budeme študovať efektívny nízko-energetický model opisujúci elektrónovú štruktúru elektrónov a Cooperovských párov [4,5] vo van der Waalsovskej heteroštruktúre feromagnetu a supravodiča.

Poznámka: Absolvent počas štúdia nadobudne teoretické vedomosti zo základov teórie tuhých látok a praktické skúsenosti počas riešenia konkrétneho problému analytickými a numerickými metódami. Získané vedomosti a praktické skúsenosti umožnia ďalší kariérny rast v akademickom prostredí.

Kľúčové slová: supravodivosť, feromagnetizmus, van der Waalsovské heteroštruktúry, materiálový výskum, nanotechnológie.

Univerzita P. J. Šafárika v Košiciach
Prírodovedecká fakulta

Vedúci: RNDr. Martin Gmitra, PhD.
Ústav : ÚFV - Ústav fyzikálnych vied
Riaditeľ ústavu: prof. RNDr. Peter Kollár, DrSc.

Spôsob sprístupnenia elektronickej verzie práce: bez obmedzenia

Dátum schválenia: 28.04.2021

Affidavit

I hereby confirm to the best of my knowledge that this thesis is solely my original work and that I have only used the sources and materials indicated.

Košice 2021 Moško . . . . . .

Acknowledgments

At this point I would like to thank the supervisor of the bachelor thesis Dr. Martin Gmitra for valuable comments and expert advice, which contributed to the elaboration of my bachelor thesis, endless patience, expertise, support and efforts to maintain morality on the board. I also thank my family and friends for their endless support and patience, care and sincere efforts to help me not only in writing my bachelor's thesis, but also in all personal areas of life.

Súhrn v štátnom jazyku

Cieľom predloženej bakalárskej práce bolo štúdium vzájomných efektov supravodivosti a magnetizmu v dvojrozmerných kryštalických systémoch tvoriacich van der Waalsovské heteroštruktúry. Hlavným záujmom bolo štúdium kvázičasticových disperzných relácií a párovacích korelačných funkcií vzhľadom na amplitúdu spinovo-orbitálnej interakcie a jej vplyv na Cooperovské párovanie elektrónov. Študovaný systém supravodič/feromagnet bol opísaný efektívnym modelom platným pre atomárne tenký supravodič $NbSe_2$, patriaci do triedy prechodových dichalkogénov (angl. transition metal dichalcogenides) s tzv. Isingovským párovaním, a polovodičový feromagnet (napr. CrI_3, $Cr_2Ge_2Te_6$). Bol preskumaný vplyv štyroch fyzikálnych parametrov na kvázičasticovú disperziu a korelačné funkcie pre Cooperove páry. Menovite bol analyzovaný chemický potenciál μ, parameter zodpovedný za spinovo-orbitálnu interakciu β_{so}, supravodivý s-vlnový singletný párovací potenciál Δ_0 a tripletný párovací potenciál Δ_{t}. Boli zistené nasledujúce skutočnosti:

1. β_{so} spôsobuje rozštiepenie energetických pásov a spinovú polarizáciu stavov.
2. Δ_0 otvára energetickú medzeru v kvázičasticovom spektre v okolí chemického potenciálu μ.
3. Δ_{t} zmenšuje energetickú medzeru singletného párovania v kvázičasticovej disperzii.

Štúdiom korelačných funkcií párovania elekrónov sme zistili, že bez singletného párovania sa v systéme nevytvárajú viazané stavy a to pri ľubovoľných podmienkach udaných zvyšnými parametrami.

Kľúčové slová: supravodivosť, van-der Waalsovská heteroštruktúra, spinovo-orbitálna interakcia, kvázi-časticová disperzia, korelačné funkcie, singletné a tripletné párovanie.

Abstract

The aim of the presented bachelor thesis was to study the mutual effects of superconductivity and magnetism in two - dimensional crystalline systems forming van der Waals heterostructures. The main interest was the study of quasiparticle dispersion relations and pairing correlation functions with respect to the amplitude of spin-orbital interaction and its influence on Cooper electron pairing. The studied superconductor / ferromagnet system was marked by an effective model valid for atomic thin superconductor $NbSe_2$, belonging to the class of transition metal dichalcogenides with the so-called Ising pairing, semiconductor ferromagnet (e.g. CrI_3, $Cr_2Ge_2Te_6$). The influence of four physical parameters on quasiparticle dispersion and correlation functions for Cooper pairs was investigated. Namely, the chemical potential μ, the parameter responsible for the spin-orbital interaction β_{so}, the superconducting s -wave singlet pairing potential Δ_0 and the triplet pairing potential Δ_{t} were analyzed. The following facts were found:

1. β_{so} splits energy bands yielding spin polarization of the states.
2. Δ_0 opens the energy gap in quasiparticle spectrum around the chemical potential μ.
3. Δ_{t} decreases the energy gap in the quasiparticle dispersion.

By studying the correlation functions of electron pairing, we have found out that without singlet pairing, no bound states are formed in the system under any of the conditions given by the remaining parameters.

Contents

List of Figures

Introduction

The purpose of the bachelor thesis is to calculate and analyse electronic structure of superconducting quasi-particles in van der Waals heterostructures of ferromagnet/superconductoran described by an effective model Hamiltonian.

In the first chapter we present description of van der Waals heterostuctures providing examples of well established systems. The basic knowledge of ferromagnetism and superconductivity is also introduced. The former one is described on the mean-field level and the later in concept of so-called BCS theory. We present features of microscopic mechanism of superconductivity by means of Cooper pair formation. Both the ferromagnetism and superconductivity are core ingredients in van der Waals heterostructures made of ferromagnetic and superconducting layers. We also discuss in details spin-orbit coupling which in van der Waals heterostuctures can play significant role on electronic band structure spin splitting and specifically can affect superconductivity via Ising pairing.

The second chapter formulates an effective model Hamiltonian relevant for single-particle states close to the Fermi level. We present extension of the Hamiltonian in Bogoliubov–de-Gennes form and derive analytical solution of the eigenvalue problem. We further analyze the quasi-particle energy dispersions and spin expectation values for selected set of parameters to demonstrate possible physical situations. We also briefly discuss Gorkov's pairing equations and correlation functions. We calculate singlet and triple pairing contributions to the correlation functions, s-wave and p-wave pairing, and present numerical results for the same set of parameters as for the quasi-particle dispersions.

1 System description and fundamental interactions

1.1 Van der Waals heterostructures

One of the most significant event in the field of condensed matter physics within the last 20 years has been demonstration of existence of atomically thin two-dimensional systems. The pioneering system is graphene discovered back to 2004 [1]. To be specific, graphene is the material with strict geometrical two-dimensional hexagonal structure possessing outstanding attributes and physical properties including high electron mobility, stiffness, spectacular electrical, chemical, and optical properties [2]. In this way, graphene is a "father" of two-dimensional materials (today we know more than 2500 other, atomically thin materials) and it launched new interest in the field of solid state. By combination via stacking of these crystals we can create new materials. In general, stacking of two-dimensional materials changes a physical properties and we can fabricate a material with novel hybrid properties. These activities open the way for designing of new materials and nano – devices [3]. It is even more fascinating we are able to gain control over the changes in yet mentioned physical attributes by the right choice of the angle by which are the independent layers rotated relative to each other what is also known as "twisting" [4].

The name van der Waals (vdW) heterostructers describes the way how are the single layers bound together to form crystal. While the in plane stability of the 2D crystal is governed by the strong covalent bonds the layers are bound via weak *van der Waals interaction* similar to how a sticky tape attaches to a flat surface. Thanks to the ubiquitous nature of vdW interactions new super-thin materials can be added together with no limitations what resembles *Lego blocks* and that is why the vdW heterostructures are sometimes called Lego-structures, see Fig. 1.1.

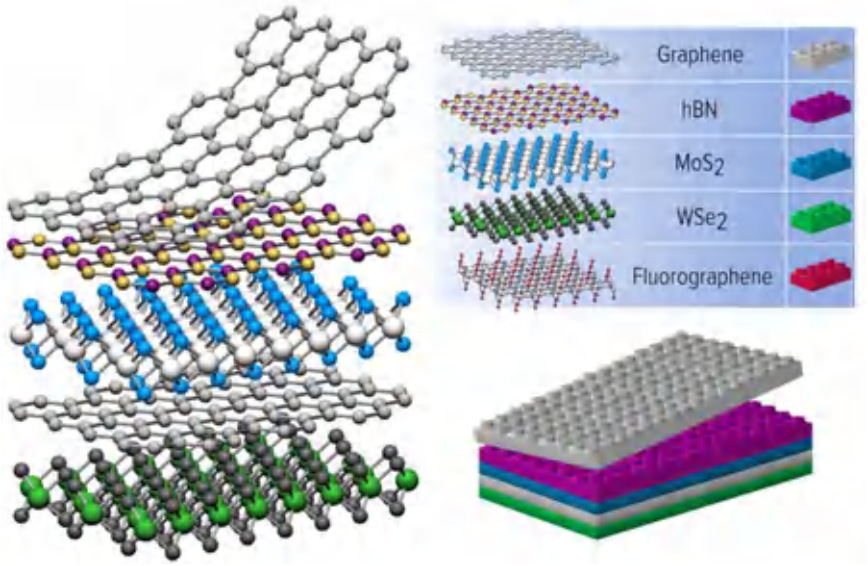

Fig. 1.1: Schematics of van der Waals heterostructures building using two-dimensional crystals (table right top) as Lego blocks (right bottom) forming a realistic atomic structures (left) allowing for construction of a huge variety of layered structures using two-dimensional crystals. Reprinted from Ref. [5].

Not so long ago, a special type of vdWs came to the attention of material scientists and nowadays known as monolayer *transition metal dichalcogenides*. Transition metal dichalcogenides (TMD) are two-dimensional materials composed of one layer of triangularly arranged transition metal atoms (e.q. Mo, Nb, W, ...) and two layers of triangularly arranged chalcogen atoms (e.g. S, Se, Te, ...) while the layer of transition atoms is sandwiched between them, see Fig. 1.2. Together they form a 2D honeycomb lattice similar to graphene but with broken sublattice symmetry [6]. Thanks to their strong mechanical properties, relatively high electron mobility and massive Dirac energy spectrum transition metal dichalcogenides are promising candidates for next generation transistors [7]. The breaking of the in-plane symmetry together with strong atomic spin-orbit coupling (SOC) results in strong Zeeman field near the $\mathbf{K}$ and $-\mathbf{K}$ valleys (corners of the first Brillouin zone). This field strongly polarizes electron spins to the out-of-plane directions and the spin polarization is an odd function with respect to the $\mathbf{K}$, therefore the direction of spin in $-\mathbf{K}$ valley is opposite to the one in $\mathbf{K}$ valley. Such a field is usually denoted as Ising SOC field.

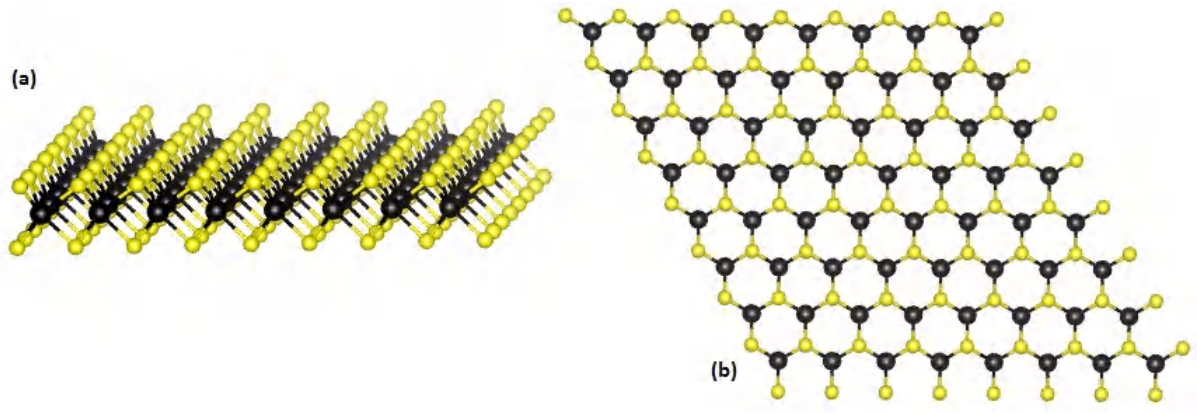

Fig. 1.2: Atomic strusture of transition metal dichalcogenide single layer. (a) side view; and (b) top view. Reproduced from Ref. [8].

Within this work we will consider a model describing low energy bands valid close to the valence or conduction band edges of any TMD, also called valleys. The model can describe, e.g., MoS_2 or $NbSe_2$ well known as Ising superconductors [9, 10, 11]. However, spin-triplet Cooper pairs can induce superconducting pairing when superconductor is in vicinity to a ferromagnet [6].

1.2 Ferromagnetism

Response of a material to an applied magnetic field define diamagnets, paramagnets and ferromagnets. For the first two, diamagnets and paramagnets, a weak response is typical. A diamagnetic material create magnetic field with opposite direction to the external field and therefore the total magnetic field in the material is "weaker" then the applied external field. A paramagnetic behaviour can be explained by an existence of atomic (also molecular or ionic) magnetic momentum which can be induced, e.g., by odd number of electrons in atom leading to unpaired atomic spin or orbital momentum. Thermal fluctuations randomize the magnetic momenta of atoms (down to zero temperature) and therefore a macroscopic magnetization is zero. However, if we apply external magnetic field, moments begin to orientate into the direction of the external magnetic field and in fact, the final magnetic field in material is "stronger" than the applied external field. With increasing magnitude of applied external field

the magnetization, which is defined as the magnetic moment per volume, increases until its value reaches the saturation magnetization $\mathbf{M}_S$. After a removal of external field, paramagentic materials are not able to sustain this enlarged field and it is once again destructed by thermal fluctuations – the material is not a permanent magnet.

The most interesting are ferromagnets. A ferromagnetic material can show a finite magnetic moment even in the absence of an external field if the temperature is below a critical temperature, the so called Curie temperature T_c. This process is carried out, if the parallel orientation of electron spins in the atoms leads to a reduction of the total energy of the system, i.e. of the exchange interaction between the spins. In other words the exchange interaction can spontaneously order the magnetic moments against the thermal fluctuations.

In order to describe a spontaneous magnetization below the T_c temperature P. -E. Weiss used a molecular field theory [12]. In his work the exchange interactions between electron spins were described by considering a free electron in the mean field of all the others. This so called "exchange field" can be written as

$$\mathbf{H}_\mathrm{xc} = \mu_0 \lambda(T) \mathbf{M} \tag{1.1}$$

where $\mathbf{M}$ represents the magnetization and the parameter λ is explicitly dependent on temperature. This idea led to the expression for the magnetic susceptibility of ferromagnets

$$\chi_\mathrm{m} = \frac{C}{T - T_\mathrm{c}} \tag{1.2}$$

which is also know as the Curie-Weiss law with a material-specific constant C [12]. The most fundamental representant of ferromagnets is iron with Curie temperature $T_\mathrm{c} = 1043$ K, beneath this temperature iron possess ferromagnetic attributes, while above it behaves as the paramagnetic material [13].

We note that recently several atomically thin two-dimensional ferromagnets were discovered and studied. For instance, CrI_3 is layered ferromagnet with Curie temperature of 61 K and 45 K for single layer [14].

1.3 Superconductivity

1.3.1. Basic properties

Superconductivity is one of the most fascinating quantum phenomenon in which electrons condensate forming pairs and flow with zero resistance. However, strong enough magnetic field can destroy the supercoductivity by breaking the electron pairs. It has been shown that superconductivity in thin films of TMD could withstand an applied magnetic field as strong as tens of Tesla due to specific Ising pairing of electrons.

Superconductivity goes back to 1908 when Heike Kamerlingh Onnes was the first to liquefy helium, using several precooling stages and the Hampson–Linde cycle based on the Joule–Thomson effect. This way he lowered the temperature to the boiling point of helium (-269 °C, 4.2 K). By reducing the pressure of the liquid helium he achieved a temperature near 1.5 K. These were the coldest temperatures achieved on earth at the time. This allows to cool down typical resistive conductor below roughly 4 K, and observe a transition where the electrical resistance ρ changed rapidly form finite value to zero [15], see Fig. 1.3.

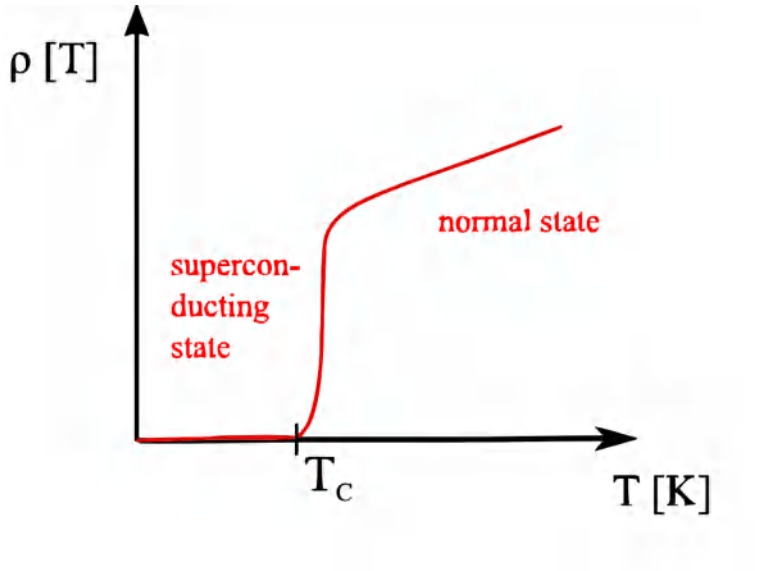

Fig. 1.3: Typical dependence of electrical resistance $\rho(T)$ of a typical conductor as a function of temperature T, changing its state to superconducting below a critical temperature T_c.

This temperature is the boundary between *normal* and *superconducting state* of material and it is also known by the term **critical temperature** T_c (distinguish the critical temperature from the magnetic transition in previous section). Similar results were shown for other alloys and metals. Later measurements shown that resistivity of superconducting materials beneath T_c has to be lower than $10^{-35}\Omega m$. This resistivity is significantly less than the resistivity of copper in extremely pure state ($\sim 10^{-12}\Omega m$). It was also shown that critical temperatures of regular superconductors are material constants and they can be found in the temperature interval $0.5\,\mathrm{K} < T_c < 20\,\mathrm{K}$. Thanks to the just mentioned attribute and phenomenon of electromagnetic induction we do possess an ability to create electric currents with relatively long lifetime. These currents are able to circulate within the superconductor for amount of time measured in hundreds of years. As it is possible to create the superconducting state of material, it is also possible to destroy it by an external magnetic field with magnitude above *critical magnetic flux density* $\mathbf{B}_c$ depending on material and temperature. For the majority of materials this dependence follows

$$B_c = B_0 \left[1 - \left(\frac{T}{T_c}\right)^2\right]. \tag{1.3}$$

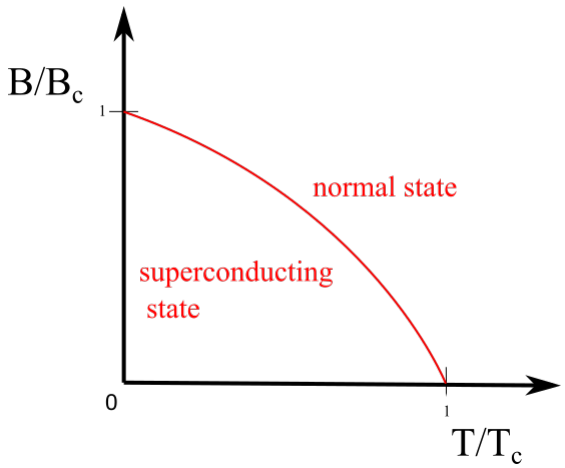

Fig. 1.4: Dependence of the magnetic flux density as a function of temperature in relative units scaled on B_c on critical magnetic flux density and critical temperature T_c.

It is quite interesting that superconducting state can be destructed by the magnetic field of it's own electric currents.The ability of perfect diamagnets to expel a magnetic field (which is

also a necessary condition of superconductivity) was proven twenty years after the discovery of superconductivity by Meissner and Oschsenfeld, see Fig. 1.5 for illustration of the diamagnetic effect of a superconductor. The magnetic flux density $\mathbf{B}$ can be calculated as

$$\mathbf{B} = \mu_0(\mathbf{H}_\mathrm{e} + \mathbf{M}), \tag{1.4}$$

where $\mathbf{M}$ stands for the magnetization of the material and $\mathbf{H}_\mathrm{e}$ is the applied external magnetic field. If we cool the probe under the critical temperature T_c, we change the state of the probe from the normal-conducting to the superconducting state and the magnetic flux gets expelled from the metal and $\mathbf{B} = 0$. If we use the Eq. (1.4), it follows

$$\mathbf{H}_\mathrm{e} = -\mathbf{M} = \chi_\mathrm{m}\mathbf{M} \tag{1.5}$$

where $\chi_\mathrm{m} = -1$ is the magnetic susceptibility which value -1 is characteristic for perfect diamagnets. This phenomenon is called *Meissner-Ochsenfeld* effect and is also well known for quantum levitation effect, where is the levitating magnet "locked" above the superconductor.

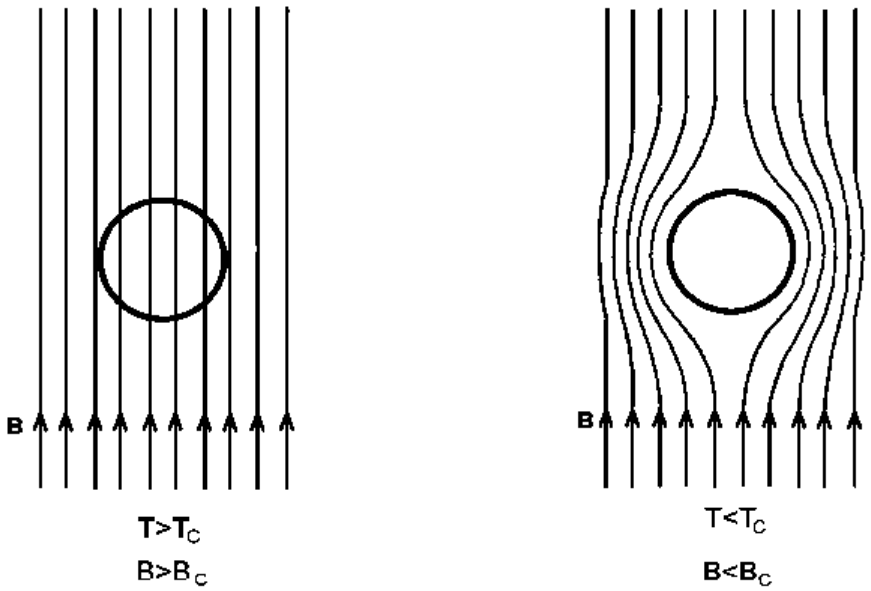

Fig. 1.5: Illustration of the Meissner effect. Magnetic flux penetrates the system in normal state (left) while it is expelled from the interior of the system (shown by the circle) in superconducting state. Reproduced from Ref. [13].

1.3.2. Theoretical description and Cooper pairs formation

John Bardeen, Leon Cooper and John Robert Schrieffer have formulated microscopic theory of superconductivity, further referred just as BCS theory [16, 17], since discovery of the superconductivity by Heike Kamerlingh Onne's in 1911. Main idea of the theory is formation of bound electron states originating a superconducting condensate.

Imagine a moving electron through a solid attracting its positive charged ions. This attraction causes lattice vibrations with low frequencies because of the fact the mass of the electron is much smaller than the one of the ions. The direct consequence of this action is the local increase of the density of positive charge towards the electron gets attracted. In the case with stronger attractive interaction than the repulsive Coulomb interaction between the electrons (this can be reached at low temperatures) an attractive interaction between the two electrons comes into play. The concept of the BCS theory elaborates on idea of formation of a BCS ground state with reduced total energy by the weak net attractive interaction between the electrons near Fermi surface of the material.[18]

Considering an electron moving through the crystal the distortions of the periodic charge density are introduced. Let us elaborate on more general concept assuming a Fermi sea where all states below the Fermi energy ε_{F} are occupied. For non-interacting electrons, the total Hamiltonian in occupation number representation formalism reads [19]

$$\hat{\mathcal{H}} = \sum_{\mathbf{k}} \sum_{\sigma} \varepsilon_{\mathbf{k}} \hat{c}^{\dagger}_{\mathbf{k},\sigma} \hat{c}_{\mathbf{k},\sigma} \,, \tag{1.6}$$

where the operator $\hat{c}^{\dagger}_{\mathbf{k},\sigma}$ is the fermion "creation operator" and it creates an electron with wave-vector $\mathbf{k}$ and spin σ, while $\hat{c}_{\mathbf{k},\sigma}$ is the corresponding annihilation operator and it destroys the corresponding electron state. The occupation number operator is defined as

$$\hat{n}_{\mathbf{k},\sigma} = \hat{c}^{\dagger}_{\mathbf{k},\sigma} \hat{c}_{\mathbf{k},\sigma}. \tag{1.7}$$

It is important to note that the total energy of the system can be obtained by the number of particles in each state multiplied by the corresponding one particle energy ε_k and finally summed over all possible momenta $\mathbf{k}$ and spin $\sigma = \pm 1$ (measured in $\left[\frac{\hbar}{2}\right]$ units). At this point the Pauli's exclusion principle requires each state $|\mathbf{k}, \sigma\rangle$ to be occupied with one electron only.

By choosing two electrons from the non-interacting Fermi sea and allowing them to occupy orbitals above E_{F} and interact through an attractive potential, one can show that these two electrons can be in a lower-energy state [20]. Consider two electrons at positions $\mathbf{r}_1$ and $\mathbf{r}_2$ with corresponding momenta $\mathbf{k}_1$ and $\mathbf{k}_2$ can be described by the planewave states

$$\Phi_{\mathbf{k}_1}(\mathbf{r}_1) = \frac{1}{\sqrt{\Omega}} e^{i\mathbf{k}_1 \cdot \mathbf{r}_1}, \quad \Phi_{\mathbf{k}_2}(\mathbf{r}_2) = \frac{1}{\sqrt{\Omega}} e^{i\mathbf{k}_2 \cdot \mathbf{r}_2}, \tag{1.8}$$

where Ω is the volume normalization. Assume now an attractive interaction between the electrons. It this case we can express wavefunction of the pair of electrons in the form

$$\psi_{\mathrm{pair}}(\mathbf{r}_1, \mathbf{r}_2) = \sum_{\mathbf{k}_1, \mathbf{k}_2} a(\mathbf{k}_1, \mathbf{k}_2) \Phi_{\mathbf{k}_1}(\mathbf{r}_1) \Phi_{\mathbf{k}_2}(\mathbf{r}_2). \tag{1.9}$$

By changing to center of mass and relative coordinates

$$\begin{aligned} \mathbf{K} &= \mathbf{k}_1 + \mathbf{k}_2 \\ \mathbf{R} &= \frac{1}{2}(\mathbf{r}_1 + \mathbf{r}_2) \\ \mathbf{k} &= \frac{1}{2}(\mathbf{k}_1 - \mathbf{k}_2) \\ \mathbf{r} &= \mathbf{r}_1 - \mathbf{r}_2 \end{aligned} \tag{1.10}$$

we have then

$$\mathbf{k}_1 \cdot \mathbf{r}_1 + \mathbf{k}_2 \cdot \mathbf{r}_2 = \mathbf{K} \cdot \mathbf{R} + \mathrm{k} \cdot \mathbf{r} \tag{1.11}$$

and

$$\psi_{\mathrm{pair}}(\mathbf{r}_1, \mathbf{r}_2) = \sum_{\mathbf{k}, \mathbf{K}} a(\mathbf{k}, \mathbf{K}) e^{i\mathbf{K} \cdot \mathbf{R}} e^{i\mathbf{k} \cdot \mathbf{r}}. \tag{1.12}$$

The total kinetic energy of the pair of electrons T is given simply by the sum of the kinetic energies of both electrons

$$T = \frac{\hbar^2 \mathbf{k}_1^2}{2m} + \frac{\hbar^2 \mathbf{k}_2^2}{2m} = \frac{\hbar^2}{m} \left[\frac{\mathbf{K}^2}{4} + \mathbf{k}^2 \right]. \tag{1.13}$$

Natural behaviour of a system is to reduce its energy. It is easy to see that the kinetic energy takes a minimal value for $\mathbf{K} = 0$

$$\frac{\partial T}{\partial \mathbf{K}} = \frac{\hbar^2 \mathbf{K}}{2m} = 0 \tag{1.14}$$

what implies

$$\mathbf{k}_1 = -\mathbf{k}_2. \tag{1.15}$$

Taking into account the fact in Eq. (1.15) the wavefunction takes the form

$$\psi_{\text{pair}}(\mathbf{r}_1,\mathbf{r}_2)=\sum_{\mathbf{k},\mathbf{K}} a(\mathbf{k},\mathbf{K})e^{i\mathbf{k}\cdot\mathbf{r}_1}e^{-i\mathbf{k}\cdot\mathbf{r}_2}\,, \tag{1.16}$$

where $a(\mathbf{k})=0$ for $\mathbf{k}<\mathbf{k}_{\text{F}}$ as the states form a degenerated Fermi system. The Schrödinger equation for the two electrons reads

$$\left(-\frac{\hbar^2}{2m}\left(\nabla_1^2+\nabla_2^2\right)\psi(\mathbf{r}_1,\mathbf{r}_2)+V(\mathbf{r}_1,\mathbf{r}_2)\right)=(E+2E_{\text{F}})\psi(\mathbf{r}_1,\mathbf{r}_2)\,, \tag{1.17}$$

where the energy E is measured from $2E_{\text{F}}$.

Let us assume $V(\mathbf{r}_1,\mathbf{r}_2)=V(\mathbf{r})$ and as we have mentioned before, refer the energy to that of two particles on the Fermi surface, then Eq. (1.17) becomes

$$-\frac{\hbar^2}{2m}\psi''(\mathbf{r})+V(\mathbf{r})\psi(\mathbf{r})=(E+2E_{\text{F}})\psi(\mathbf{r}) \tag{1.18}$$

Using expresion for the wavefunction in Eq. (1.16) and defining

$$\epsilon_{\mathbf{k}}=\frac{\hbar^2k^2}{2m}-E_{\text{F}},\quad V_{\mathbf{k},\mathbf{k}'}=\langle\mathbf{k}|\,V\left|\mathbf{k}'\right\rangle, \tag{1.19}$$

we obtain the Bethe–Goldstone equation [21]

$$\sum_{\mathbf{k}'}V_{\mathbf{k},\mathbf{k}'}a(\mathbf{k})=(E-2\epsilon_{\mathbf{k}})a(\mathbf{k}) \tag{1.20}$$

where we sum over all $\mathbf{k}'\neq\mathbf{k}$. The last equation describes the scattering of a pair $(\mathbf{k},-\mathbf{k})\rightarrow(\mathbf{k}',-\mathbf{k}')$.

At this point one arrives to the oncoming question – What should be in general the sign of the potential $V_{\mathbf{k},\mathbf{k}'}$? If $V_{\mathbf{k},\mathbf{k}'}$ is attractive, we obviously expect that the electrons may bind in pairs. By chose $V_{\mathbf{k},\mathbf{k}'}$ to be attractive and being constant over the energy range from zero to some energy level E_{D} measured from the Fermi energy E_{F}

$$V_{\mathbf{k},\mathbf{k}'}=\begin{cases}-V/\Omega & \epsilon_{\mathbf{k}},\epsilon_{\mathbf{k}'}<E_{\text{D}}\\ 0 & \text{otherwise.}\end{cases} \tag{1.21}$$

By using the assumption in Eq. (1.21) we can rewrite the Eq. (1.20) as follows

$$(E-2\epsilon_{\mathbf{k}})a(\mathbf{k})=-\frac{V}{\Omega}\sum_{\mathbf{k}'}a(\mathbf{k}'), \tag{1.22}$$

and

$$a(\mathbf{k}) = \frac{c}{E - 2\epsilon_{\mathbf{k}}} \tag{1.23}$$

for all $|\mathbf{k}| > k_{\mathrm{F}}$. Here c is the constant $c = -\frac{V}{\Omega}\sum_{\mathbf{k}'} a(\mathbf{k}')$ and has to be obtained self-consistently including the energy E

$$c = -\frac{V}{\Omega}\sum_{\mathbf{k}'} \frac{c}{E - 2\epsilon_{\mathbf{k}'}}\,. \tag{1.24}$$

To sum up over the states one can use density of states $N(\epsilon)$

$$1 = V\int_a^{E_{\mathrm{D}}} \frac{N(\epsilon)}{2\epsilon - E} d\epsilon\,, \tag{1.25}$$

where the density of states $N(\epsilon) \approx N(0)$ which allows to perform integration yielding

$$E = -\frac{2E_{\mathrm{D}}}{e^{\frac{2}{N(0)V}} - 1}\,. \tag{1.26}$$

In case of weak coupling where $N(0)V \ll 1$, we obtain

$$E = -2E_{\mathrm{D}} e^{-\frac{2}{N(0)V}}\,. \tag{1.27}$$

For strong coupling, $N(0)V \gg 1$ on the other hand

$$E = -E_{\mathrm{D}} N(0) V. \tag{1.28}$$

If we consider the case of the weak coupling and measure the energy of the two electron state from zero level, we obtain

$$\epsilon \approx 2\epsilon_{\mathrm{F}} - 2\hbar\omega_0 \exp\left(-\frac{1}{VN(\epsilon_{\mathrm{F}})}\right), \tag{1.29}$$

where the second term is also known as *superconducting gap* [22, 15]

$$\Delta_0 = 2\hbar\omega_0 \exp\left\{-\frac{1}{VN(\varepsilon_F)}\right\}. \tag{1.30}$$

Existence of the superconducting gap is a result of attractive interactions between electrons close to the Fermi surface which leads to the formation of energetically more stable two-electron states, Cooper pairs.

1.4 Spin-orbit coupling

The spin-orbit coupling (SOC) is a relativistic effect caused by the interaction of a particle's spin with its motion inside a potential. A classical example is a shift in an electron's atomic energy levels, caused by the electromagnetic interaction between the electron's magnetic dipole, its orbital motion, and the electrostatic field of the positively charged nucleus. This leads in splitting of spectral lines, which can be interpreted as an analogy to the Zeeman effect, as a consequence of two relativistic effects: the apparent magnetic field seen from the electron perspective and the magnetic moment of the electron associated with its intrinsic spin [23].

To start from a more theoretical point of view, one should have a closer look at the SOC Hamiltonian

$$\hat{\mathcal{H}}_{\mathrm{SOC}} = \frac{e\hbar}{4m^2c^2}\sigma \cdot (\mathbf{E} \times \hat{\mathbf{p}}), \tag{1.31}$$

which can be extracted from the Pauli equation [24]

$$\left[\frac{p^2}{2m} + V + \frac{e\hbar}{2m}\sigma \cdot \mathbf{B} - \frac{e\hbar\sigma \cdot \mathbf{p} \times \mathbf{E}}{4m^2c^2} - \frac{e\hbar^2}{8m^2c^2}\nabla \cdot \mathbf{E} - \frac{p^4}{8m^3c^2} - \frac{e\hbar p^2}{4m^3c^2}\sigma \cdot \mathbf{B} - \frac{(e\hbar B)^2}{8m^3c^2}\right] |\psi\rangle = E\,|\psi\rangle\,, \tag{1.32}$$

for electrons without external magnetic fields as a relativistic correction. The meaning of the symbols used is as follows $\mathbf{E}$ denotes to electric field intensity, $\mathbf{B}$ is the magnetic flux density, $\sigma = (\sigma_x, \sigma_y, \sigma_z)^T$ refers to vector of Pauli matrices, $\hat{\mathbf{p}} = -i\hbar\nabla$ is the momentum operator, m is the particle mass and q is the charge of the particle.

In general electrical field $\mathbf{E}$ includes internal fields as well as external ones caused by an applied gate voltage. In solid structures the electrons are also affected by the average periodic crystal potential. Accordingly, SOC reveals the symmetry of the crystal lattice and the eigenstates of the Hamiltonian $\hat{\mathcal{H}}_{\mathrm{SOC}}$ must obey **Bloch's theorem**. As the SOC introduces mixing of spins, the eigenstates of the Hamiltonian $\hat{\mathcal{H}}_{\mathrm{SOC}}$ can be written in the following form [25]

$$|\psi\rangle_{n,\mathbf{k},\uparrow}(r) = [a_{n,\mathbf{k}}(r)\,|\uparrow\rangle + b_{n,\mathbf{k}}(r)\,|\downarrow\rangle]e^{i\mathbf{k}\cdot\mathbf{r}} \tag{1.33}$$

and

$$|\psi\rangle_{n,\mathbf{k},\downarrow}(r) = [a^*_{n,-\mathbf{k}}(r)\,|\downarrow\rangle - b^*_{n,-\mathbf{k}}(r)\,|\uparrow\rangle]e^{i\mathbf{k}\cdot\mathbf{r}}. \tag{1.34}$$

As we can see, both the eigenstates are written as a superposition of spin states $|\uparrow\rangle$ and $|\downarrow\rangle$ relative to a chosen quantization axis [26] with band indices n and wave vector $\mathbf{k}$. SOC is in general a weak interaction, therefore we expect the lattice−periodic parameters to fulfill

$$|a_{n,\mathbf{k}}| \approx 1 \gg |b_{n,\mathbf{k}}| \tag{1.35}$$

and according to this assumption it is possible to call the states in Eqs. (1.33) and (1.34) **effective spin up** ($\Uparrow$) and **effective spin down** ($\Downarrow$) states.

If we use the time reversal operator for spin-1/2 particles

$$\hat{T} = -i\sigma_y \hat{C}\,, \tag{1.36}$$

where $\hat{C}$ is the operator for complex conjugation, it is possible to prove the time reversal invariance of the $\hat{H}_{\mathrm{SOC}}$ Hamiltonian. The direct consequence of this feature is the same energy eigenvalues according to Kramer's theorem [27] of effective spin up state $|\psi\rangle_{n,\mathbf{k},\uparrow}$ and its time-reversed

$$\hat{T}\,|\psi\rangle_{n,\mathbf{k},\uparrow}(\mathbf{r}) = \left[a^*_{n,\mathbf{k}}(r)\,|\downarrow\rangle - b^*_{n,\mathbf{k}}(r)\,|\uparrow\rangle\right] e^{i\mathbf{k}\cdot\mathbf{r}}. \tag{1.37}$$

In order to better understand the physical meaning of the SOC, consider a material with and without spatial symmetry. For a centro-symmetric material that contains space inversion point, we can easily replace the $\mathbf{k}$ by the $-\mathbf{k}$ and this change will not change the physical properties of the assumed state and it's time reversed state. In this case the effective spin up and spin down states possess the same energy eigenvalues what implies the degeneracy of the energy bands.

In case of materials without spatial symmetry the SOC typically leads to the broken twofold spin degeneracy except the so-called time-reversal invariant points symmetry points. This is the reason why is the SOC field usually interpreted as k-dependent Zeeman-like field [28, 29]. In such a case the related Hamiltonian can be written as

$$\mathcal{H}_{\mathrm{SOC}} = \mathbf{\Omega}(\mathbf{k}) \cdot \sigma. \tag{1.38}$$

As the SOC preserves the time reversal, the spin-orbit field $\mathbf{\Omega}(\mathbf{k})$ has to be an odd function in momentum $\mathbf{k}$. However we should note the fact that the analogy is not complete. The main difference between the Zeeman effects and SOC is that SOC preserves time-reversal

symmetry. Accordingly, the band splitting caused by SOC has nothing to do with the rise of a net magnetization in the assumed material. In the case of our problem the model Hamiltonian for SOC takes on the form [6]

$$\mathcal{H}_{\mathrm{SOC}} = \varepsilon \beta_{\mathrm{so}} \sigma_z \,, \tag{1.39}$$

where the condition of time reversal symmetry enters via ε (valley index) which possesses value $\varepsilon = 1$ for the $\mathbf{K}$ valley and $\varepsilon = -1$ for the $-\mathbf{K}$ valley. In this sense the $\mathcal{H}_{\mathrm{SOC}}$ stays odd in $\mathbf{k}$.

2 Problem formulation and Results

2.1 Hamiltonian of the system

Recently discovered superconductivity in thin films of TMD can survive strong magnetic fields up to 40 Tesla [10, 9]. An explanation originates from a specific lattice structure of the TMD that allows the moving electrons in the material to experience strong internal magnetic fields of about 100 Tesla. This special type of internal magnetic fields emerge from spin-orbit coupling and instead of damaging superconductivity it protects the superconducting electron pairs from being broken. Such type of superconductors are called *Ising superconductors*. The pairing mechanism has been soon observed in others TMD systems having similar lattice structure, such as $NbSe_2$ [11] without need of heavy liquid gating of MoS_2 [10]. This suggest that the bands near the Fermi level need to be filled. In TMD systems the Fermi surface is specifically appeared in vicinity of the so called **K**-valleys (edges of the first Brillouin zone). We note that these energy bands originate mainly from the transition metal d_{z^2} orbitals.

In order to describe the electronic states close to the Fermi level we introduce an effective Hamiltonian near the **K** and $-\mathbf{K}$ valleys describing single particle states in the basis of $(c_{k\uparrow},c_{k\downarrow})$

$$\mathcal{H}_0(\mathbf{k}=\mathbf{p}+\varepsilon\mathbf{K}) = \left(\frac{|p|^2}{2m}-\mu\right)\sigma_0 + \varepsilon\beta_{\mathrm{so}}\sigma_z\,, \tag{2.1}$$

where **K** stands for the wave-vector of the K-point, $\varepsilon = \pm 1$ is the index of the the valley, **p** represents the momentum measured from the K or $-K$ points, μ is the chemical potential, β_{so} is the spin-orbit coupling strength responsible for spin pinning in z-direction referred also as Ising spin-orbit coupling and

$$\sigma_0 = \begin{pmatrix} 1 & 0 \\ 0 & 1 \end{pmatrix}, \sigma_z = \begin{pmatrix} 1 & 0 \\ 0 & -1 \end{pmatrix}, \tag{2.2}$$

are the Pauli matrices. Finally the Hamiltonian can be written in the matrix form as follows

$$\mathcal{H}_0(\mathbf{k}=\mathbf{p}+\varepsilon\mathbf{K}) = \begin{pmatrix} \frac{p^2}{2m}+\varepsilon\beta_{\mathrm{so}}-\mu & 0 \\ 0 & \frac{p^2}{2m}-\varepsilon\beta_{\mathrm{so}}-\mu \end{pmatrix}. \tag{2.3}$$

The spin close to the **K** valleys is quantized in out-of-plane direction (z-axis). The origin of the β_{so} term can be explained by the coupling between the transition metal d-orbitals and p-orbitals of chalcogen atoms [30]. This coupling is responsible for the broken in-plane mirror symmetry in the material and therefore it pins the electron spins to the out-of-plane directions. Such an effect can be viewed as a valley resolved Zeeman field related to the Ising spin-orbit coupling.

To investigate superconductivity in TMD we follow standard procedure of mean field Bogoliubov-de-Gennes approach [31] and use the Hamiltonian H_0 given in Eq. (2.3) to write the effective quasiparticle Hamiltonian in the Nambu basis $(c_{\mathbf{k}\uparrow}, c_{\mathbf{k}\downarrow}, c^{\dagger}{}_{-\mathbf{k}\uparrow}, c^{\dagger}{}_{-\mathbf{k}\downarrow})$

$$\mathcal{H}_{\mathrm{BdG}}(\mathbf{k}) = \begin{pmatrix} H_0(\mathbf{k}) & \Delta_0 i\sigma_y \\ -\Delta_0 i\sigma_y & -{H_0}^*(-\mathbf{k}) \end{pmatrix}, \tag{2.4}$$

where σ_y is the Pauli matrice

$$\sigma_y = \begin{pmatrix} 0 & -i \\ i & 0 \end{pmatrix}, \tag{2.5}$$

and Δ_0 is the spin-singlet *s-wave pairing* potential. The Boguliubov-de-Gennes Hamiltonian in vicinity of the **K** valley takes a form of the 4×4 matrix

$$\mathcal{H}_{\mathrm{BdG}}(\mathbf{p}+\mathbf{K}) = \begin{pmatrix} \frac{p^2}{2m}+\beta_{\mathrm{so}}-\mu & 0 & 0 & \Delta_0 \\ 0 & \frac{p^2}{2m}-\beta_{\mathrm{so}}-\mu & -\Delta_0 & 0 \\ 0 & -\Delta_0 & -\frac{p^2}{2m}-\beta_{\mathrm{so}}+\mu & 0 \\ \Delta_0 & 0 & 0 & -\frac{p^2}{2m}+\beta_{\mathrm{so}}+\mu \end{pmatrix} \tag{2.6}$$

and in the $-\mathbf{K}$ valley it reads

$$\hat{\mathcal{H}}_{\mathrm{BdG}}(\mathbf{p}-\mathbf{K}) = \begin{pmatrix} \frac{p^2}{2m}-\beta_{\mathrm{so}}-\mu & 0 & 0 & \Delta_0 \\ 0 & \frac{p^2}{2m}+\beta_{\mathrm{so}}-\mu & -\Delta_0 & 0 \\ 0 & -\Delta_0 & -\frac{p^2}{2m}+\beta_{\mathrm{so}}+\mu & 0 \\ \Delta_0 & 0 & 0 & -\frac{p^2}{2m}-\beta_{\mathrm{so}}+\mu \end{pmatrix}. \tag{2.7}$$

We note that momentum and wave vector are related through the de Broglie relation $\mathbf{p} = \hbar\mathbf{k}$. By solving the time independent Schrödinger equation for the Boguliubov-de-Gennes Hamiltonian Eqs. (2.6) and (2.7) we obtain the quasiparticles energy spectrum near the $\pm\mathbf{K}$ valleys

$$\begin{pmatrix} E^1_{\mathbf{p}+\varepsilon\mathbf{K}} \\ E^2_{\mathbf{p}+\varepsilon\mathbf{K}} \\ E^3_{\mathbf{p}+\varepsilon\mathbf{K}} \\ E^4_{\mathbf{p}+\varepsilon\mathbf{K}} \end{pmatrix} = \begin{pmatrix} -\varepsilon\beta_{\mathrm{so}} - Q_0/2m \\ \varepsilon\beta_{\mathrm{so}} - Q_0/2m \\ -\varepsilon\beta_{\mathrm{so}} + Q_0/2m \\ \varepsilon\beta_{\mathrm{so}} + Q_0/2m \end{pmatrix}, \tag{2.8}$$

where $Q_0 = \sqrt{p^4 + 4m^2\Delta_0^2 - 4m\mu p^2 + 4m^2\mu^2}$, and the corresponding normalized eigenstates read

$$\left|\psi^1_{\mathbf{p}+\varepsilon\mathbf{K}}\right\rangle = \begin{pmatrix} 0 \\ -\frac{P_0}{2m\Delta_0\sqrt{1+\frac{1}{4}\left[\frac{P_0}{m\Delta_0}\right]^2}} \\ \frac{1}{\sqrt{1+\frac{1}{4}\left[\frac{P_0}{m\Delta 0}\right]^2}} \\ 0 \end{pmatrix}, \qquad \left|\psi^2_{\mathbf{p}+\varepsilon\mathbf{K}}\right\rangle = \begin{pmatrix} -\frac{-P_0}{2m\Delta_0\sqrt{1+\frac{1}{4}\left[\frac{-P_0}{m\Delta_0}\right]^2}} \\ 0 \\ 0 \\ \frac{1}{\sqrt{1+\frac{1}{4}\left[\frac{-P_0}{m\Delta_0}\right]^2}} \end{pmatrix},$$

$$\left|\psi^3_{\mathbf{p}+\varepsilon\mathbf{K}}\right\rangle = \begin{pmatrix} 0 \\ -\frac{P_0}{2m\Delta_0\sqrt{1+\frac{1}{4}\left[\frac{P_0}{m\Delta_0}\right]^2}} \\ \frac{1}{\sqrt{1+\frac{1}{4}\left[\frac{P_0}{m\Delta_0}\right]^2}} \\ 0 \end{pmatrix}, \qquad \left|\psi^4_{\mathbf{p}+\varepsilon\mathbf{K}}\right\rangle = \begin{pmatrix} -\frac{-P_0}{2m\Delta_0\sqrt{1+\frac{1}{4}\left[\frac{-P_0}{m\Delta_0}\right]^2}} \\ 0 \\ 0 \\ \frac{1}{\sqrt{1+\frac{1}{4}\left[\frac{-P_0}{m\Delta_0}\right]^2}} \end{pmatrix}, \tag{2.9}$$

where $P_0 = p^2 - 2m\mu + Q_0$.

As we have already mentioned, the Ising SOC pins the electron spins to the out-of-plane direction. This can be easily seen for calculated spin expectation values. In order to calculate

spin projections we span the spin operators in the basis of Pauli matrices

$$\sigma_{z_\mathrm{e}} = \frac{1}{2}(\sigma_0 + \sigma_z) \otimes \sigma_z = \begin{pmatrix} 1 & 0 & 0 & 0 \\ 0 & -1 & 0 & 0 \\ 0 & 0 & 0 & 0 \\ 0 & 0 & 0 & 0 \end{pmatrix} \tag{2.10}$$

$$\sigma_{x_\mathrm{e}} = \frac{1}{2}(\sigma_0 + \sigma_z) \otimes \sigma_x = \begin{pmatrix} 0 & 1 & 0 & 0 \\ 1 & 0 & 0 & 0 \\ 0 & 0 & 0 & 0 \\ 0 & 0 & 0 & 0 \end{pmatrix}, \tag{2.11}$$

$$\sigma_{y_\mathrm{e}} = \frac{1}{2}(\sigma_0 + \sigma_z) \otimes \sigma_y = \begin{pmatrix} 0 & -i & 0 & 0 \\ i & 0 & 0 & 0 \\ 0 & 0 & 0 & 0 \\ 0 & 0 & 0 & 0 \end{pmatrix}. \tag{2.12}$$

Analogically we have defined spanned Pauli matrices for holes

$$\sigma_{z_\mathrm{h}} = \frac{1}{2}(\sigma_0 - \sigma_z) \otimes \sigma_z = \begin{pmatrix} 0 & 0 & 0 & 0 \\ 0 & 0 & 0 & 0 \\ 0 & 0 & 1 & 0 \\ 0 & 0 & 0 & -1 \end{pmatrix}, \tag{2.13}$$

$$\sigma_{x_\mathrm{h}} = \frac{1}{2}(\sigma_0 - \sigma_z) \otimes \sigma_x = \begin{pmatrix} 0 & 0 & 0 & 0 \\ 0 & 0 & 0 & 0 \\ 0 & 0 & 0 & 1 \\ 0 & 0 & 1 & 0 \end{pmatrix}, \tag{2.14}$$

$$\sigma_{y_\mathrm{h}} = \frac{1}{2}(\sigma_0 - \sigma_z) \otimes \sigma_y = \begin{pmatrix} 0 & 0 & 0 & 0 \\ 0 & 0 & 0 & 0 \\ 0 & 0 & 0 & -i \\ 0 & 0 & i & 0 \end{pmatrix}, \tag{2.15}$$

where $\otimes$ is the Kronecker product of two matrices. The expectation values of spin projections of electron and hole states were calculated according to the definition of the quantum mechanical

observable

$$\left\langle \hat{A} \right\rangle = \langle \psi | \, \hat{A} \, | \psi \rangle = \int_{-\infty}^{\infty} \psi^* \hat{A} \psi \, \mathrm{d}x. \tag{2.16}$$

The spin expectation values for the electron in units of $\hbar/2$ read

$$\begin{pmatrix} \left\langle \hat{S}_{z_\eta}(\left|\psi_{\mathbf{p}+\varepsilon\mathbf{K}}\right\rangle^1) \right\rangle \\ \left\langle \hat{S}_{z_\eta}(\left|\psi_{\mathbf{p}+\varepsilon\mathbf{K}}\right\rangle^2) \right\rangle \\ \left\langle \hat{S}_{z_\eta}(\left|\psi_{\mathbf{p}+\varepsilon\mathbf{K}}\right\rangle^3) \right\rangle \\ \left\langle \hat{S}_{z_\eta}(\left|\psi_{\mathbf{p}+\varepsilon\mathbf{K}}\right\rangle^4) \right\rangle \end{pmatrix} = \begin{pmatrix} -\frac{4(\eta-1)+(\eta+1)P_0^2/(m\Delta_0)^2}{8R_0} \\ \frac{4(\eta-1)+(\eta+1)P_0^2/(m\Delta_0)^2}{8R_0} \\ -\frac{4(\eta-1)+(\eta+1)P_1^2/(m\Delta_0)^2}{8R_1} \\ \frac{4(\eta-1)+(\eta+1)P_1^2/(m\Delta_0)^2}{8R_1} \end{pmatrix}, \tag{2.17}$$

where $\eta = \pm 1$ for electrons and holes, respectively, $P_1 = p^2 - 2m\mu + Q_0$, $R_0 = 1 + (P_0/m\Delta_0)^2/4$, and $R_1 = 1 + (P_1/m\Delta_0)^2/4$. The in-plane spin components are found to be zero

$$\begin{pmatrix} \left\langle \hat{S}_{x_\eta}(\left|\psi_{\mathbf{p}+\varepsilon\mathbf{K}}\right\rangle^1) \right\rangle \\ \left\langle \hat{S}_{x_\eta}(\left|\psi_{\mathbf{p}+\varepsilon\mathbf{K}}\right\rangle^2) \right\rangle \\ \left\langle \hat{S}_{x_\eta}(\left|\psi_{\mathbf{p}+\varepsilon\mathbf{K}}\right\rangle^3) \right\rangle \\ \left\langle \hat{S}_{x_\eta}(\left|\psi_{\mathbf{p}+\varepsilon\mathbf{K}}\right\rangle^4) \right\rangle \end{pmatrix} = \begin{pmatrix} \left\langle \hat{S}_{y_\eta}(\left|\psi_{\mathbf{p}+\varepsilon\mathbf{K}}\right\rangle^1) \right\rangle \\ \left\langle \hat{S}_{y_\eta}(\left|\psi_{\mathbf{p}+\varepsilon\mathbf{K}}\right\rangle^2) \right\rangle \\ \left\langle \hat{S}_{y_\eta}(\left|\psi_{\mathbf{p}+\varepsilon\mathbf{K}}\right\rangle^3) \right\rangle \\ \left\langle \hat{S}_{y_\eta}(\left|\psi_{\mathbf{p}+\varepsilon\mathbf{K}}\right\rangle^4) \right\rangle \end{pmatrix} = \begin{pmatrix} 0 \\ 0 \\ 0 \\ 0 \end{pmatrix}. \tag{2.18}$$

2.2 p-wave superconducting pairing

The p-wave pairing can be effectively described extending the s-wave pairing considering an additional non-diagonal term in the Boguliubov–de-Gennes Hamiltonian [32]. In this sense one introduces the spin-triplet potential Δ_t generalizing the superconducting gap parameter [33]. The gap term $\Delta_0 i\sigma_y$ is extended to the form $(\Delta_0 + \Delta_\mathrm{t}\sigma_z)i\sigma_y$, and the Hamiltonian takes the form

$$\hat{\mathcal{H}}_\mathrm{BdG} = \begin{pmatrix} \frac{p^2}{2m} - \mu + \varepsilon\beta_\mathrm{so} & 0 & 0 & \Delta_0 + \Delta_\mathrm{t} \\ 0 & \frac{p^2}{2m} - \mu - \varepsilon\beta_\mathrm{so} & -\Delta_0 + \Delta_\mathrm{t} & 0 \\ 0 & -\Delta_0 - \Delta_\mathrm{t} & -\frac{p^2}{2m} + \mu - \varepsilon\beta_\mathrm{so} & 0 \\ \Delta_0 - \Delta_\mathrm{t} & 0 & 0 & -\frac{p^2}{2m} + \mu + \varepsilon\beta_\mathrm{so} \end{pmatrix}. \tag{2.19}$$

The eigenvalues and eigenvectors of this Hamiltonian are obtained analogically as in the previous section and they acquire the form

$$\begin{pmatrix} E^1_{\mathbf{p}+\varepsilon\mathbf{K}} \\ E^2_{\mathbf{p}+\varepsilon\mathbf{K}} \\ E^3_{\mathbf{p}+\varepsilon\mathbf{K}} \\ E^4_{\mathbf{p}+\varepsilon\mathbf{K}} \end{pmatrix} = \begin{pmatrix} -\varepsilon\beta_{\mathrm{so}} - Q_{\mathrm{t}}/2m \\ \varepsilon\beta_{\mathrm{so}} - Q_{\mathrm{t}}/2m \\ -\varepsilon\beta_{\mathrm{so}} + Q_{\mathrm{t}}/2m \\ \varepsilon\beta_{\mathrm{so}} + Q_{\mathrm{t}}/2m \end{pmatrix}, \tag{2.20}$$

where $Q_{\mathrm{t}} = \sqrt{p^4 + 4m^2\Delta_0^2 - 4m^2\Delta_{\mathrm{t}}^2 - 4m\mu p^2 + 4m^2\mu^2}$. The eigenstates read

$$\left|\psi^1_{\mathbf{p}+\varepsilon\mathbf{K}}\right\rangle = \begin{pmatrix} 0 \\ \frac{-P_{\mathrm{t}_2}}{2m\Delta\sqrt{1+\frac{1}{4}\left[\frac{P_{\mathrm{t}_2}}{m\Delta}\right]^2}} \\ \frac{1}{\sqrt{1+\frac{1}{4}\left[\frac{P_{\mathrm{t}_2}}{m\Delta}\right]^2}} \\ 0 \end{pmatrix}, \qquad \left|\psi^2_{\mathbf{p}+\varepsilon\mathbf{K}}\right\rangle = \begin{pmatrix} \frac{P_{\mathrm{t}_2}}{2m\Delta\sqrt{1+\frac{1}{4}\left[\frac{-P_{\mathrm{t}_2}}{m\Delta}\right]^2}} \\ 0 \\ 0 \\ \frac{1}{\sqrt{1+\frac{1}{4}\left[\frac{-P_{\mathrm{t}_2}}{m\Delta}\right]^2}} \end{pmatrix},$$

$$\left|\psi^3_{\mathbf{p}+\varepsilon\mathbf{K}}\right\rangle = \begin{pmatrix} \frac{P_{\mathrm{t}_1}}{2m\Delta\sqrt{1+\frac{1}{4}\left[\frac{-P_{\mathrm{t}_1}}{m\Delta}\right]^2}} \\ 0 \\ 0 \\ \frac{1}{\sqrt{1+\frac{1}{4}\left[-\frac{P_{\mathrm{t}_1}}{m\Delta}\right]^2}} \end{pmatrix}, \qquad \left|\psi^4_{\mathbf{p}+\varepsilon\mathbf{K}}\right\rangle = \begin{pmatrix} 0 \\ \frac{-P_{\mathrm{t}_1}}{2m\Delta\sqrt{1+\frac{1}{4}\left[\frac{P_{\mathrm{t}_1}}{m\Delta}\right]^2}} \\ \frac{1}{\sqrt{1+\frac{1}{4}\left[\frac{P_{\mathrm{t}_1}}{m\Delta}\right]}} \\ 0 \end{pmatrix}, \tag{2.21}$$

where we have defined $\Delta = \Delta_0 + \Delta_{\mathrm{t}}$, $P_{\mathrm{t}_1} = p^2 - 2m\mu + Q_{\mathrm{t}}$ and $P_{\mathrm{t}_2} = p^2 - 2m\mu - Q_{\mathrm{t}}$.

In the limit $\Delta_{\mathrm{t}} \to 0$ both the wavefunctions and the energy dispersions reduced to the case discussed in the previous section. Further we will investigate effect of Δ_{t} on the quasiparticle energy spectrum and spin expectation value projected to the z-axis.

2.3 Quasiparticle spectra analysis

In this section we analyse results obtained in previous sections 2.1 and 2.2. We plot the quasiparticle dispersions and the spin expectation values for electrons and holes and explore their dependencies on set of values for the superconducting spin-singlet s-wave pairing potential Δ_0, spin-triple p-wave pairing potential Δ_t, Ising SOC parameter β_{so} and chemical potential μ. For the parameters we consider physically relevant values not exceeding 1 meV. In the following discussion of the spin expectation values we use the same color as for the quasiparticle energy dispersions and the corresponding color scale is set to describe variation of the spin in the interval from $-\hbar/2$ to $\hbar/2$. We analyse the case of $\varepsilon = 1$ (in vicinity of the **K** valley).

In Fig. 2.1 we show dispersion in normal state $\Delta_0 = \Delta_t \to 0$ for the case without spin-orbit coupling, $\beta_{so} = 0$ eV, and chemical potential set to zero, $\mu = 0$ eV. The electron and hole dispersions are spin degenerate and touch at the valley. Calculated $\langle S_{z_e} \rangle$ is equal zero for holes, while for the electrons get full polarization.

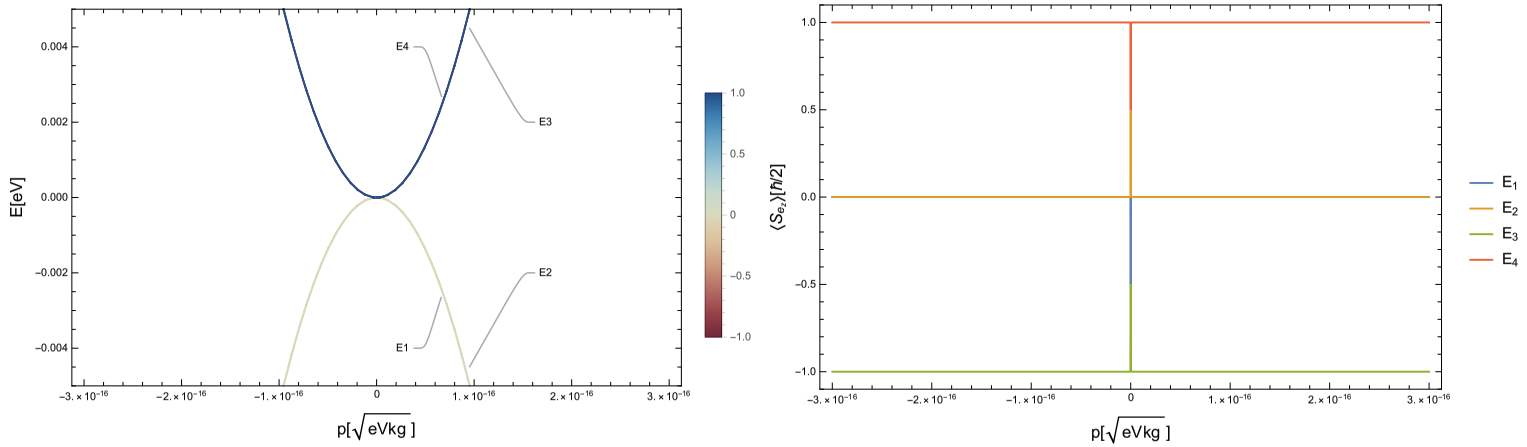

Fig. 2.1: Calculated quasiparticle dispersion (left) and spin expectation values $\langle S_{z_e} \rangle$ (right) for $\beta_{so} = 0$ eV, $\mu = 0$ eV, and $\Delta_0 = \Delta_t \to 0$, colored according to states.

In the next step we discuss effect of the β_{so} parameter on the quasiparticle dispersion in the normal state. Figure 2.2 shows dispersion that are split by the Ising SOC field. The bands preserve their spin and are fully polarized in case of electrons, see right panel in Fig. 2.2.

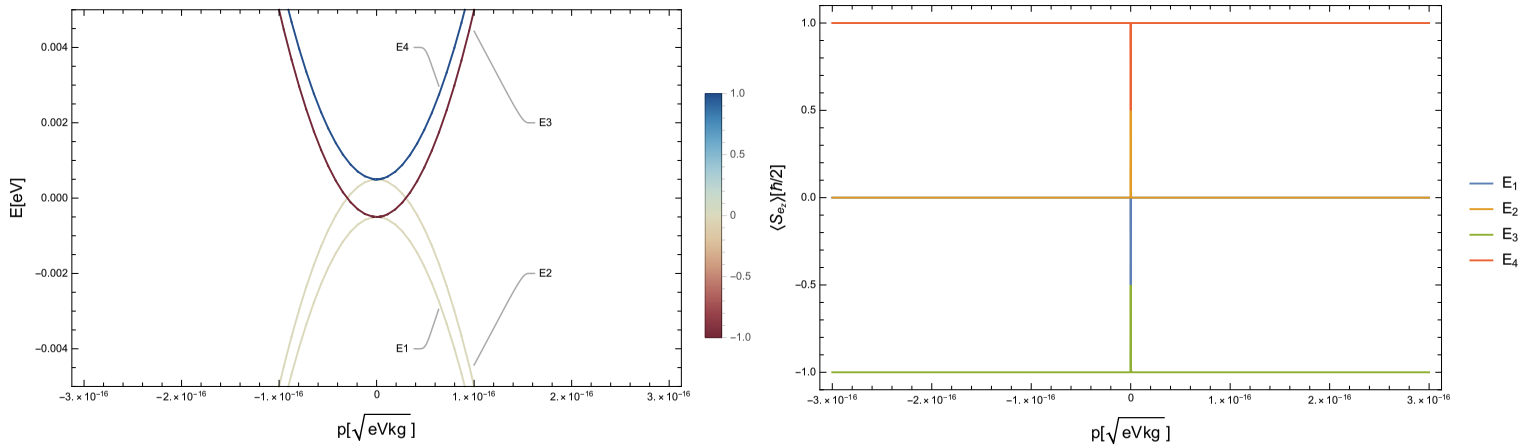

Fig. 2.2: Calculated quasiparticle dispersion and spin expectation values as in Fig. 2.2 for $\beta_{\mathrm{so}} = 0.5 \cdot 10^{-4}$ eV, $\mu = 0$ eV, and $\Delta_0 = \Delta_{\mathrm{t}} \to 0$.

Now we discuss effect of the chemical potential μ on the dispersion in normal state. Chemical potential controls level of system doping or position of the Fermi level. In the case of the quasiparticle picture non-zero chemical potential shifts the electron and hole branches towards each other.

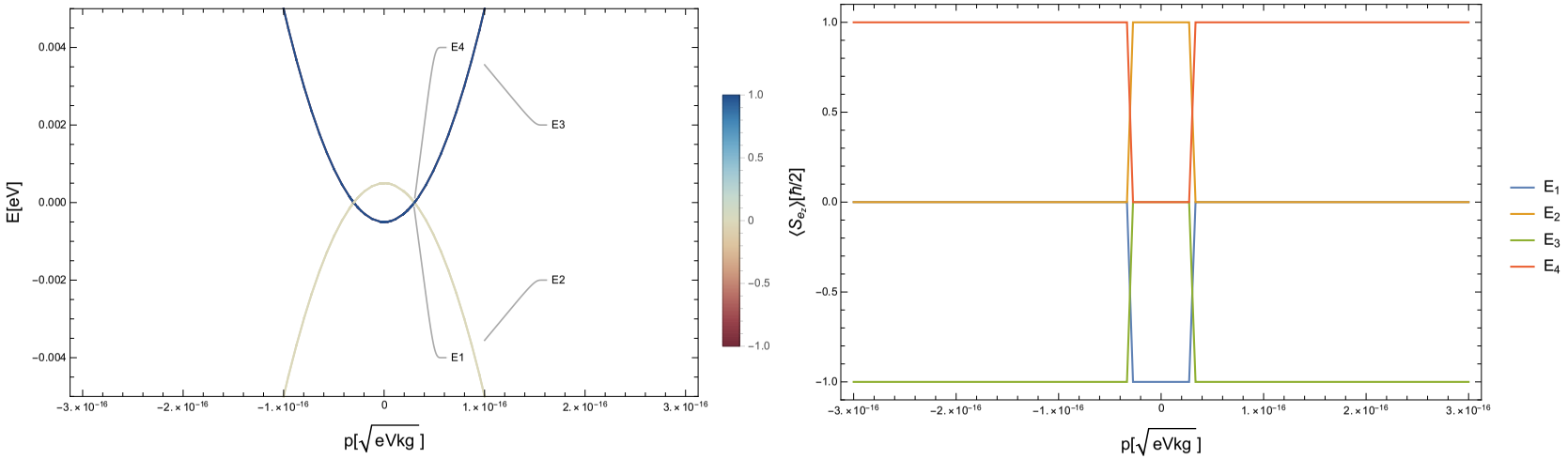

Fig. 2.3: Calculated quasiparticle dispersion and spin expectation values as in Fig. 2.2 for $\beta_{\mathrm{so}} = 0$ eV, $\mu = 0.5 \cdot 10^{-4}$ eV, and $\Delta_0 = \Delta_{\mathrm{t}} \to 0$.

Considering now superconducting state, $\Delta_0 \neq 0$, a global spectral gap is opened. In case of non-zero spin-orbit coupling the bands are spin split and spectral gap is shrunk. In Fig. 2.4 we show quasiparticle dispersions in superconducting state and spin expectation values for electrons in case of finite spin-orbit coupling and chemical potential. In the case we chose equal values for $\beta_{\mathrm{so}} = \mu = \Delta_0$ which leads to band touching near the **K** in which the spin changes sign. In this way the electron spin is transferred to hole branches due to spin-singlet pairing.

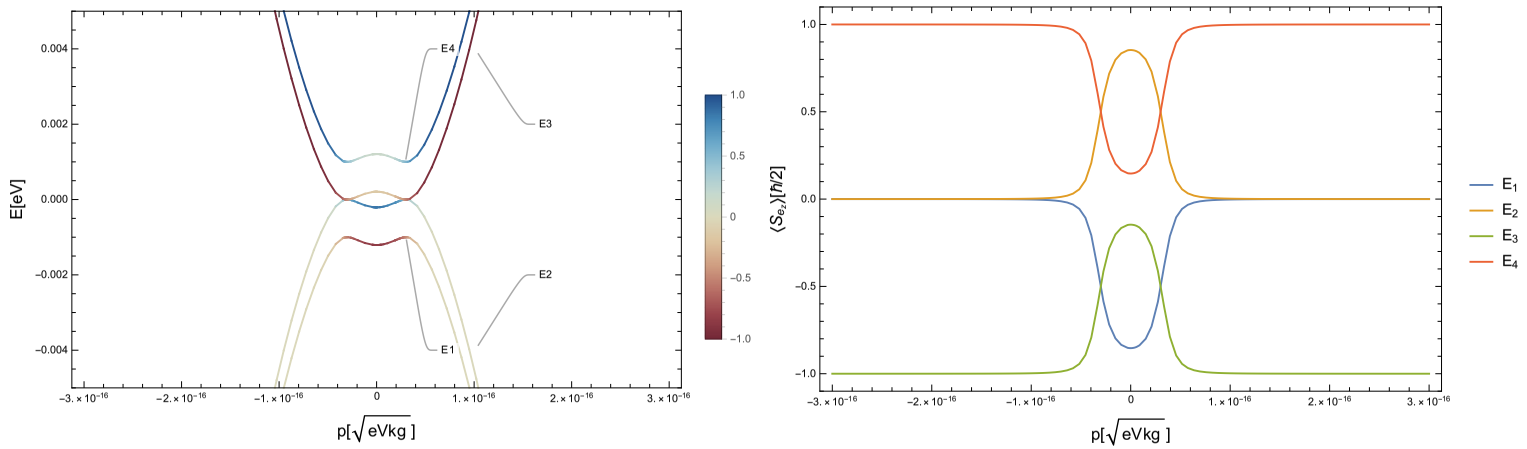

Fig. 2.4: Calculated quasiparticle dispersion (left) and spin expectation values $\langle S_{z_e} \rangle$ (right) for $\beta_{\mathrm{so}} = 0.5 \times 10^{-4}$ eV, $\mu = 0.5 \times 10^{-4}$ eV, $\Delta_0 = 0.5 \times 10^{-4}$ eV, and $\Delta_{\mathrm{t}} = 0$. The dispersions are colored according electron spin expectation value $\langle S_{z_e} \rangle$.

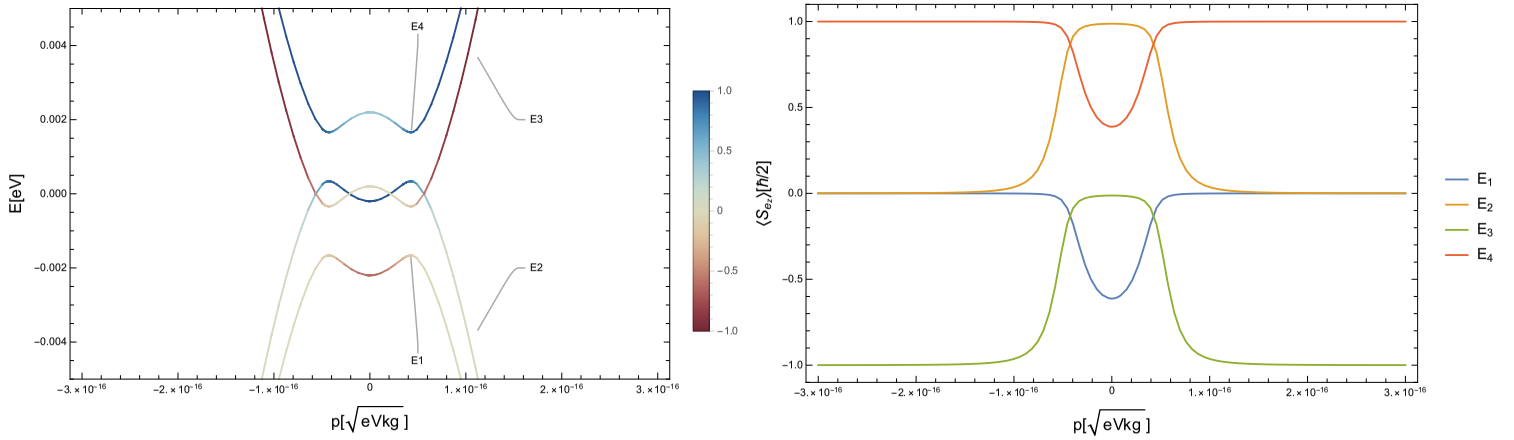

Fig. 2.5: Calculated quasiparticle dispersion (left) and spin expectation values $\langle S_{z_e} \rangle$ (right) for parameters as in Fig. 2.4 but for $\Delta_{\mathrm{t}} = 2.5 \cdot 10^{-4}$ eV.

Consider now Hamiltonian given by expression (2.19) with non-zero spin-triplet pairing. Main effect of the Δ_t potential on the quasiparticle dispersion is that the inner spin-split bands are further mixed. However, the overall effect on the dispersion can be seen as both the spin split electron and hole branches are shift in energy according to their spin, similar to Zeeman shift, see Fig. 2.5.

2.4 Pairing correlations of Cooper pairs

To investigate pairing symmetry of the Cooper pairs one solves the Gor'kov equations [34] to obtain the pairing correlations. The pairing correlations are defined as follows

$$F_{\alpha\beta}(\mathbf{k},E) = -i\int_0^\infty e^{i\left(E+i0^+\right)}\left\langle\left\{c_{\mathbf{k},\alpha}(t), c_{-\mathbf{k},\beta}(0)\right\}\right\rangle dt\,, \tag{2.22}$$

where α and β are particle's spin. Using H_{BdG} Hamiltonian in Eq. (2.6) and expressing the pairing correlations in the matrix form we can write

$$F(\mathbf{k},E) = \Delta_0\left[\psi(\mathbf{k},E)\sigma_0 + \mathbf{d}(\mathbf{k},E)\cdot\sigma\right] i\sigma_y\,, \tag{2.23}$$

where ψ describes the spin-singlet pairing correlation and $\mathbf{d}$ is a vector parametrizes the spin-triplet pairing. In the case of Ising superconductor the orientation of $\mathbf{d}$ is parallel to the z-axis (perpendicular to the film plane), therefore, we can write $\mathbf{d} = (0,0,d_z)$. Near the $\mathbf{K}$ valleys one finds [6]

$$\psi(\mathbf{p}+\varepsilon\mathbf{K},E) = \frac{E_+^2 - \Delta_0^2 - \xi_{\mathbf{p}}^2 - \beta_{\mathrm{so}}^2}{M(\mathbf{p},E_+)} \tag{2.24}$$

$$d_z(\mathbf{p}+\varepsilon\mathbf{K},E) = \frac{2\varepsilon\beta_{\mathrm{so}}\xi_{\mathbf{p}}}{M(\mathbf{p},E_+)} \tag{2.25}$$

where

$$\xi_{\mathbf{p}} = \frac{|\mathbf{p}|^2}{2m} - \mu, \quad M(\mathbf{p},E) = (\Delta_0^2 + \xi_{\mathbf{p}}^2 - E^2)^2 + 2\beta_{\mathrm{so}}^2(\Delta_0^2 - \xi_{\mathbf{p}}^2 - E^2)^2 + \beta_{\mathrm{so}}^4, \quad E_0 = E + i0^+. \tag{2.26}$$

Up to now we have considered the s-wave pairing. To include the p-wave pairing we introduce the p-wave pairing potential Δ_{t} enhancing the d_z term having the form

$$d_z(\mathbf{p},E) = \frac{\Delta_{\mathrm{t}}P(\mathbf{p},E_+) + 2\varepsilon\beta_{\mathrm{so}}\xi_{\mathbf{p}}\Delta_0}{Q_+(\mathbf{p},E_+)Q_-(\mathbf{p},E_+)}. \tag{2.27}$$

Here

$$P(\mathbf{p},E) = \Delta_0^2 - \Delta_{\mathrm{t}}^2 - \xi_{\mathbf{p}}^2 - 4\beta_{\mathrm{so}}^2 + E^2\,, \tag{2.28}$$

$$Q_+(\mathbf{p},E) = (\Delta_0 + \Delta_{\mathrm{t}})^2 + (\xi_{\mathbf{p}} + \varepsilon\beta_{\mathrm{so}})^2 - E^2\,, \tag{2.29}$$

$$Q_-(\mathbf{p},E) = (\Delta_0 - \Delta_{\mathrm{t}})^2 + (\xi_{\mathbf{p}} - \varepsilon\beta_{\mathrm{so}})^2 - E^2\,, \tag{2.30}$$

where $\varepsilon = \pm 1$ denotes the valley-index and $E_+ = E + i0^+$. After substituting into the previous expressions we get

$$\psi(\mathbf{p}+\varepsilon\mathbf{K}, E) = \frac{-\beta_{\mathrm{so}}^2 - \Delta_0^2 - \left(\frac{p^2}{2m} - \mu\right)^2 + E^2}{\beta_{\mathrm{so}}^4 + 2\beta_{\mathrm{so}}^2\left(\Delta_0^2 - \left(\frac{p^2}{2m} - \mu\right)^2 - E^2\right) + \left(\Delta_0^2 + \left(\frac{p^2}{2m}\right)^2 - E^2\right)}, \tag{2.31}$$

$$d_z(\mathbf{p}+\varepsilon\mathbf{K}, E) = \frac{2\beta_{\mathrm{so}}\Delta_0\varepsilon\left(\frac{p^2}{2m} - \mu\right) + \Delta_{\mathrm{t}}\left(-4\beta_{\mathrm{so}}^2 + \Delta_0^2 - \Delta_{\mathrm{t}}^2 - \left(\frac{p^2}{2m} - \mu\right)^2 + E^2\right)}{\left((\Delta_0 - \Delta_{\mathrm{t}})^2 + \left(-\varepsilon\beta_{\mathrm{so}} - \mu + \frac{p^2}{2m}\right)^2 - E^2\right)\left((\Delta_0 - \Delta_{\mathrm{t}})^2 + \left(\varepsilon\beta_{\mathrm{so}} - \mu + \frac{p^2}{2m}\right)^2 - E^2\right)}. \tag{2.32}$$

The pairing correlation functions for electrons for a given spin can be obtained by multiplying the matrix in equation (2.23) by the eigenvectors of the effective Hamiltonian in equation (2.4) by appropriate combination of spinors. After some algebra we obtain

$$F_{-+}(\mathbf{p}+\varepsilon\mathbf{K}, E) = \Delta_0\left(\frac{-\beta_{\mathrm{so}}^2 - \Delta_0^2 - \left(\frac{p^2}{2m} - \mu\right)^2 + E^2}{\beta_{\mathrm{so}}^4 + 2\beta_{\mathrm{so}}^2\left(\Delta_0^2 - \left(\frac{p^2}{2m} - \mu\right)^2 - E^2\right) + \left(\Delta_0^2 + \left(\frac{p^2}{2m}\right)^2 - E^2\right)^2}\right) +$$
$$+\Delta_0\left(\frac{2\beta_{\mathrm{so}}\Delta_0\varepsilon\left(\frac{p^2}{2m} - \mu\right)\Delta_{\mathrm{t}}\left(-4\beta_{\mathrm{so}}^2 + \Delta_0^2 - \Delta_{\mathrm{t}}^2 - \left(\frac{p^2}{2m} - \mu\right)^2 + E^2\right)}{\left((\Delta_0 - \Delta_{\mathrm{t}})^2 + \left(-\varepsilon\beta_{\mathrm{so}} - \mu + \frac{p^2}{2m}\right)^2 - E^2\right)\left((\Delta_0 - \Delta_{\mathrm{t}})^2 + \left(\varepsilon\beta_{\mathrm{so}} - \mu + \frac{p^2}{2m}\right)^2 - E^2\right)}\right), \tag{2.33}$$

and

$$F_{+-}(\mathbf{p}+\varepsilon\mathbf{K}, E) = -\Delta_0\left(\frac{-\beta_{\mathrm{so}}^2 - \Delta_0^2 - \left(\frac{p^2}{2m} - \mu\right)^2 + E^2}{\beta_{\mathrm{so}}^4 + 2\beta_{\mathrm{so}}^2\left(\Delta_0^2 - \left(\frac{p^2}{2m} - \mu\right)^2 - E^2\right) + \left(\Delta_0^2 + \left(\frac{p^2}{2m}\right)^2 - E^2\right)^2}\right) +$$
$$+\Delta_0\left(\frac{2\beta_{\mathrm{so}}\Delta_0\varepsilon\left(\frac{p^2}{2m} - \mu\right)\Delta_{\mathrm{t}}\left(-4\beta_{\mathrm{so}}^2 + \Delta_0^2 - \Delta_{\mathrm{t}}^2 - \left(\frac{p^2}{2m} - \mu\right)^2 + E^2\right)}{\left((\Delta_0 - \Delta_{\mathrm{t}})^2 + \left(-\varepsilon\beta_{\mathrm{so}} - \mu + \frac{p^2}{2m}\right)^2 - E^2\right)\left((\Delta_0 - \Delta_{\mathrm{t}})^2 + \left(\varepsilon\beta_{\mathrm{so}} - \mu + \frac{p^2}{2m}\right)^2 - E^2\right)}\right). \tag{2.34}$$

In the following we analyse the pairing correlations for electrons and holes considering set of parameters analysed in the previous section. Pairing correlations are functions of energy and momentum representing the affinity of the particles with a certain momentum, energy

and spin to create bound states (Cooper pairs), either singlet or triplet states. The correlation functions extend relatively large range of values, therefore, we plotted them as color maps in logarithmic scale.

Similarly as in the previous section we analyze effect of the parameters β_{so}, μ and Δ_0 on the pairing correlations while we initially set $\Delta_{\mathrm{t}} = 0$ eV. According to the definition of d_z, F_{-+} and F_{+-} for this particular case it is obvious that d_z acquires zero values if at least one of the parameter β_{so} or Δ_0 is equal to zero, and F_{-+}, F_{+-} are zero for single pairing Δ_0=0. Therefore we plot just the function ψ for each of the independent change in the decisive parameters and the case with all the parameters equal to zero. The case with $\Delta_0 \neq 0$ will be analysed separately (see Fig. 2.7a).

We start to analyze the ψ function characterizing spin-singlet pairing correlations varying β_{so}, μ and Δ_0 independently. According to the definition of ψ function Eq. (2.31) the spin-singlet pairing functions do not depend on ε, so the visualised calculations are valid for both valleys. From dependence shown in Fig. 2.6a one can conclude that the spin-singlet pairing is non-zero even for all of the parameters are equal to zero.

Pairing correlation function ψ in the presence of non-zero μ in normal state is shown in Fig. 2.6d. One sees that the curvature of the not yet opened gap (the gap is opened by $\Delta_0 \neq 0$) is the same as the in the quasiparticle dispersion (Fig. 2.3). Interestingly, the area between the electron and hole dispersions possesses negative values of ψ which implies relatively low probability to find the spin-singlet bound states in this area.

The fact, that the change in Δ_0 parameter opens the superconducting gap in the quasiparticle dispersion is also reflected in Fig. 2.6c, where ψ follows quasiparticle dispersion dependencies where inside the energy there correlation is minimal suggesting minimal presence of the paired states.

The last of the independent changes of parameters is related to the spin-orbit coupling β_{so} parameter. The singlet pairing correlation function ψ is shown in Fig. 2.6b. Dependence of the ψ function also follows the quasiparticle dispersion, see Fig. 2.2, while it possess negative values in the areas close to the individual energy bands and in the area between the intersecting lines.

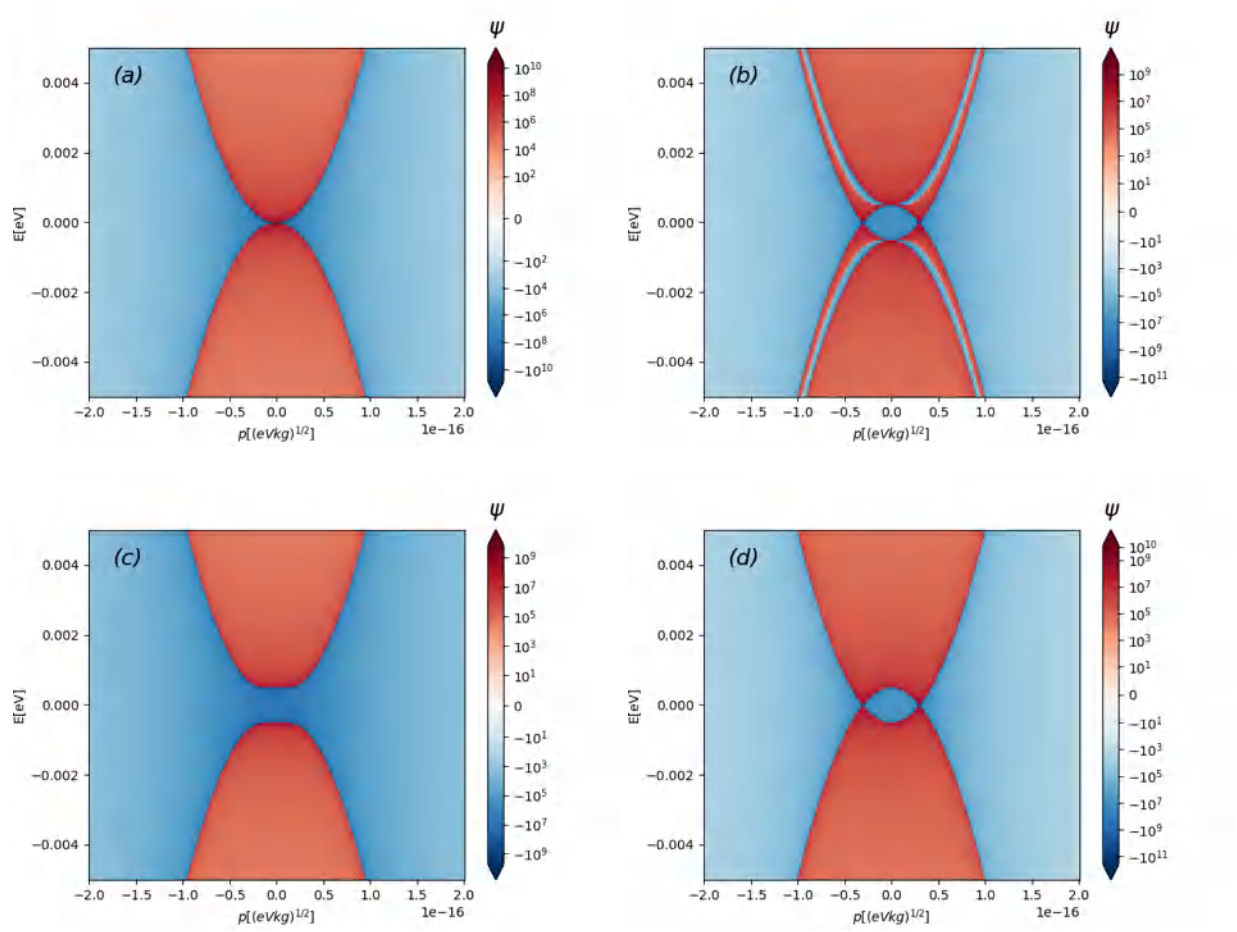

Fig. 2.6: Calculated spin-singlet pairing correlations as a function of quasiparticle energy and momentum for (a) $\beta_{\mathrm{so}} = \Delta_0 = \mu = 0$; (b) $\beta_{\mathrm{so}} = 5 \cdot 10^{-4}$ eV, $\Delta_0 = \mu = 0$,; (c) $\Delta_0 = 5 \cdot 10^{-4}$ eV, $\beta_{\mathrm{so}} = \mu = 0,1$; (d) $\mu = 5 \cdot 10^{-4}$ eV, $\beta_{\mathrm{so}} = \Delta_0 = 0$.

In following we analyse effect of the Δ_0 parameter on the pairing correlations. Specific feature of the Δ_0 parameter is the way it contributes to the final pairing correlation. While $\Delta_0 = 0$ the correlation functions for electrons and holes possess zero values independently of other parameters. Non-zero Δ_0 parameter will no cause the dependence of pairing correlations on ε and therefore the calculated properties are once again valid for both valleys.

In Fig. 2.7 we show pairing properties for non-zero spin-singlet potential Δ_0 and zero spin-orbit coupling. In this case the spectral gap between the electrons and holes is opened as shows function ψ, see Fig. 2.7a. Spin-triplet pairing is zero, see Fig. 2.7b, confirming obviously that it is impossible to get spin-triplet correlations for only $\Delta_0 \neq 0$. Functions F_{-+} and F_{+-}

are formed just by the ψ function having opposite sign, compare Fig. 2.7a, and Fig. 2.7c and 2.7d.

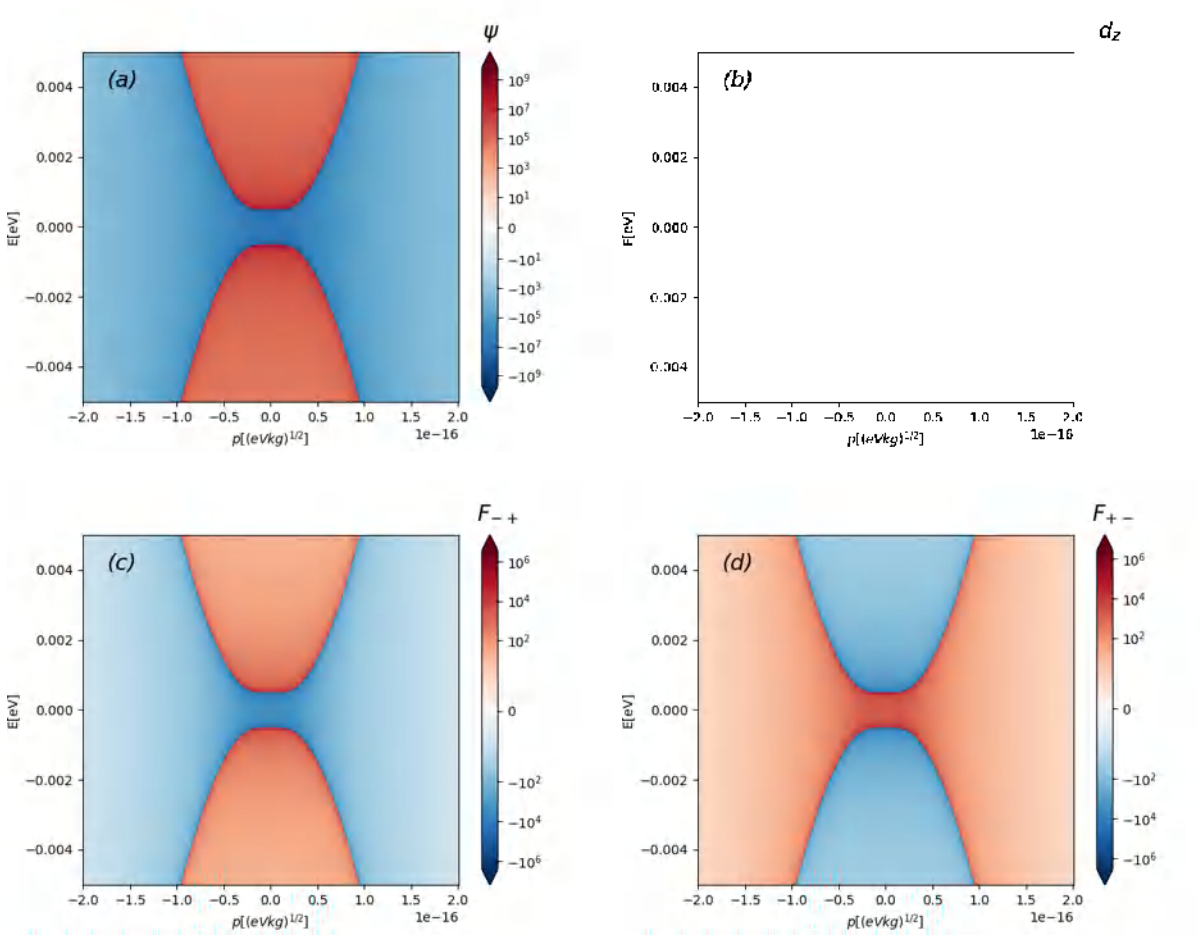

Fig. 2.7: Calculated Cooper pairing properties as a function of quasiparticle energy and momentum. (a) spin singlet pairing ψ in units $(\mathrm{eV})^{-2}$; (b) spin triplet pairing d_z in $(\mathrm{eV})^{-2}$; (c) pairing correlation components F_{-+}; and (d) F_{+-} in $(\mathrm{eV})^{-1}$ for $\Delta_0 = 5 \cdot 10^{-4}$ eV, $\beta_{\mathrm{so}} = \mu = \Delta_{\mathrm{t}} = 0$.

Now we consider the case of non-zero parameters μ, Δ_0, β_{so} but we still hold $\Delta_{\mathrm{t}} = 0$ eV. The uniqueness of this case if compared to the previous situations is in the non-zero values of the d_z function responsible for the spin-triplet pairing, see Fig. 2.8a, taking into account all of the parameters. One can easily detect the effects of the Δ_0 and β_{so} parameters which are common to ψ while it also possesses individual behaviour represented by relatively high pairing within the vertical strip located in the center of the gap. Of interest is also the positive value

of ψ within the gap which contributes together with the d_z, see Fig. 2.8b, to the final non-zero pairing correlation inside the gap. The pairing correlations shown in Fig. 2.8c and Fig. 2.8d reflect opposite sign valued spin-singlet correlations ψ due to zero spin-triplet potential. None of the calculated properties depends on ε in this situation.

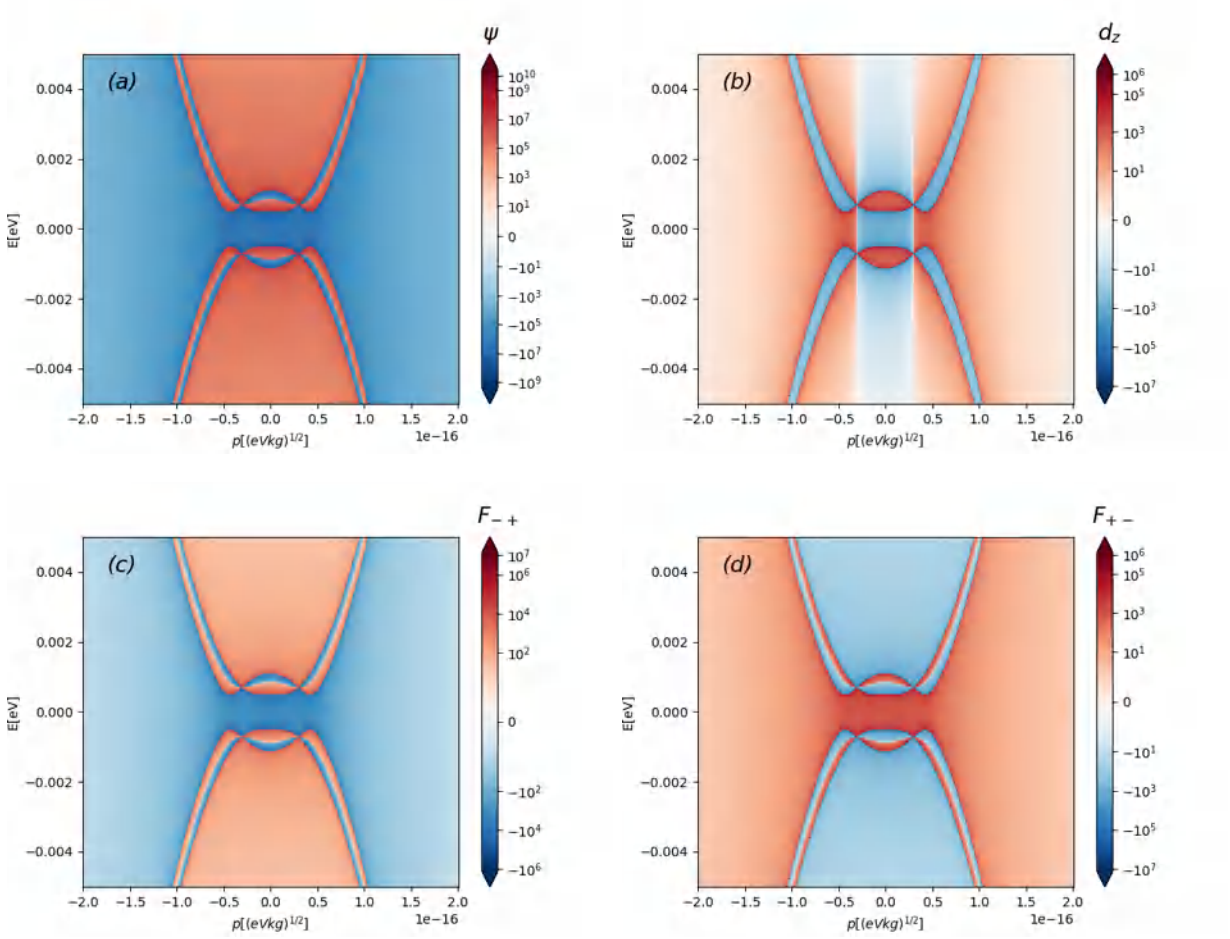

Fig. 2.8: Calculated properties of Cooper pairing for quasiparticle energy and momentum as in Fig. 2.7 for $\Delta_0 = \beta_{so} = \mu = 5 \cdot 10^{-4}$ eV and $\Delta_t = 0$.

The last of the discussed cases in the previous section is the situation with $\Delta_t < \Delta_0$. In general the results obtained by the change of Δ_t are very diverse. In order to demonstrate some particular results we have chosen a set of parameters $\beta_{so} = 5 \cdot 10^{-4}$ eV, $\mu = 5 \cdot 10^{-4}$ eV, $\Delta_0 = 5 \cdot 10^{-4}$ eV and $\Delta_t = 2.5 \cdot 10^{-4}$ eV. The functions d_z, ψ and pairing correlations F_{-+}, F_{+-} are shown in Fig. (2.9a), (2.9b), (2.9c) and (2.9d). The most interesting change is observed in the d_z function. It still reflects the basic effects of the first three independent parameters

while it also possess some effects bound to the Δ_t parameter. The ψ_s function is not explicitly nor implicitly dependent on the Δ_t parameter which implies no changes while we alter the Δ_t. Finally the pairing correlations F_{-+} and F_{+-} point to the fact the spin-triplet pairing in this case is much weaker than the spin-singlet pairing and its contribution to the pairing correlations is relatively small.

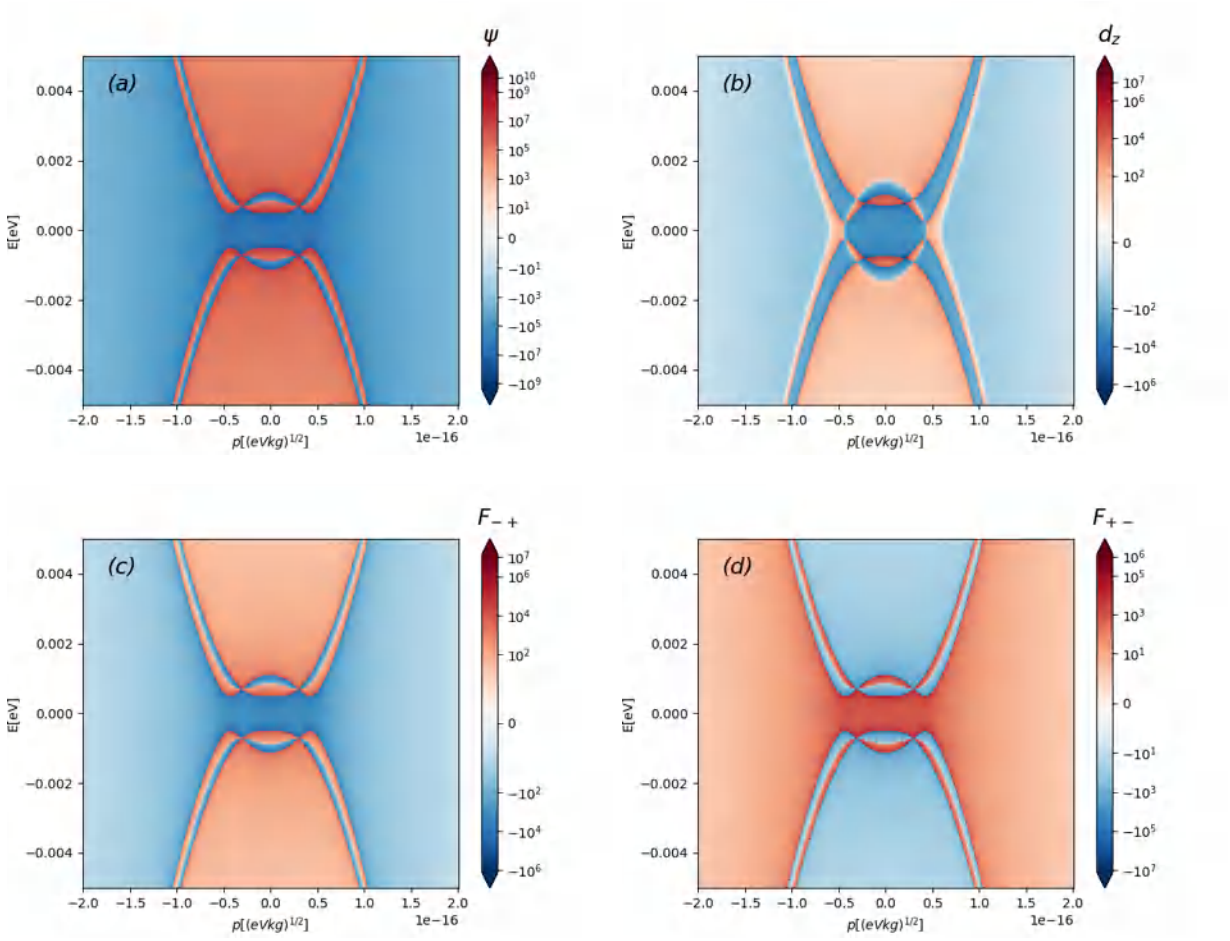

Fig. 2.9: Calculated properties of Cooper pairing for quasiparticle energy and momentum as in Fig. 2.8 but for $\Delta_t = 2.5 \cdot 10^{-4}$ eV and $\varepsilon = 1$.

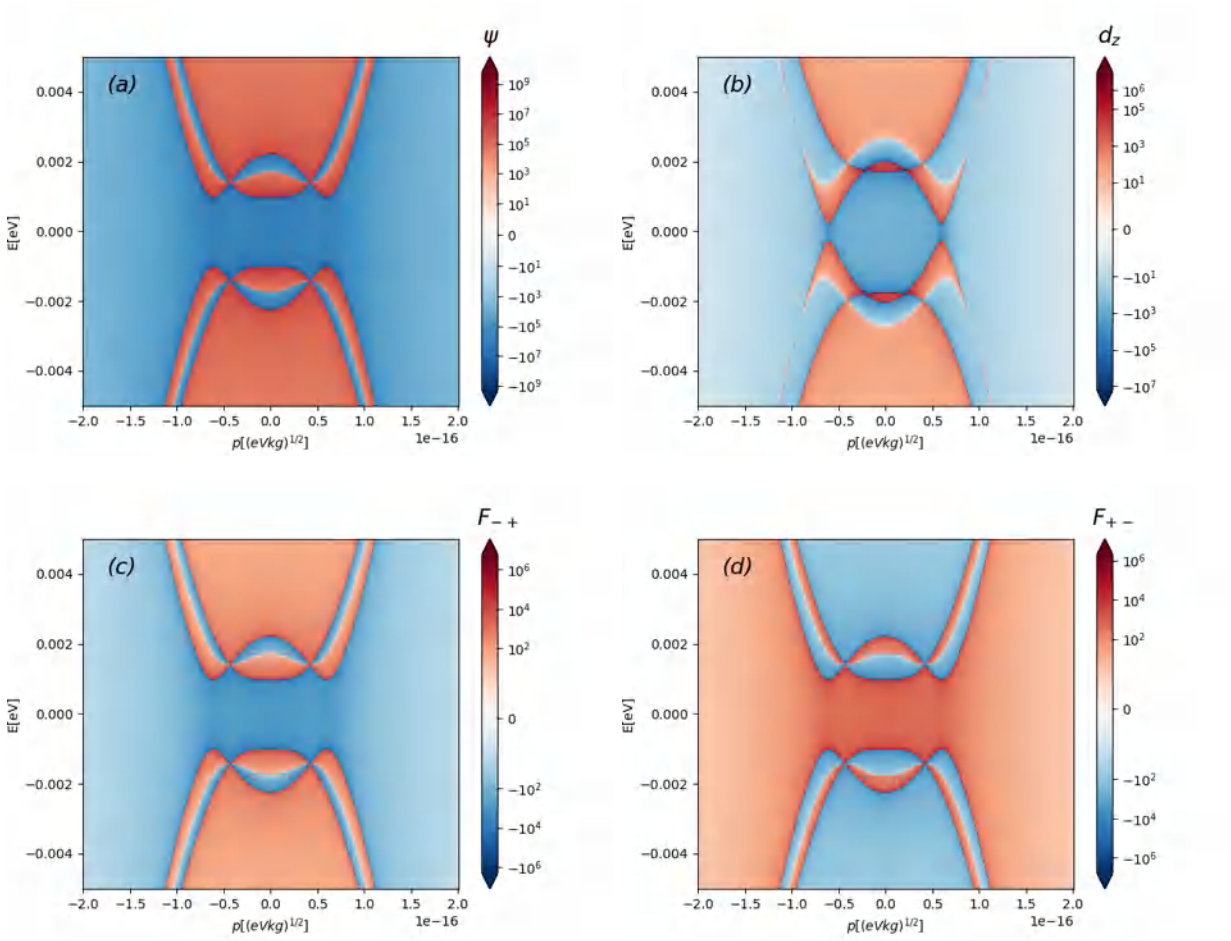

Fig. 2.10: Calculated properties of Cooper pairing for quasiparticle energy and momentum as in Fig. 2.9 for $\Delta_t = 7.5 \cdot 10^{-4}$ eV.

To enrich the concept of spin-triplet pairing we have decided to explore one more situation with the values of parameters $\beta_{so} = 10^{-3}$ eV, $\mu = 10^{-3}$ eV, $\Delta_0 = 10^{-3}$ eV and $\Delta_t = 5 \cdot 10^{-4}$ eV. In this case the d_z function shown in Fig. 2.10b captures exotic effect of p-pairing not pronouncedly seen in correlation functions F_{-+}, see Fig. 2.10c and F_{+-}, see Fig. 2.10d.

3 Conclusion and Outlook

In the thesis we investigated mutual effect of superconductivity and magnetism in two-dimensional crystalline systems forming van der Waals heterostructures. We concentrated our interest on the case of out-of-plane spin quantization axis for pairing of electrons parallel to the magnetization of a ferromagnet. The main interest was focused on study of the quasiparticle dispersion relations and pairing correlation functions with respect to the amplitude of spin-orbit interaction and its influence on Cooper electron pairing. In section 2.3 we have investigated effect of the model parameters on quasiparticle dispersion relations selecting representative physical cases.

Correlation effects which contains information on pairing of electrons within Cooper pairs were studied in section 2.4. We examined the correlations first for individual parameter changes, described their effect on singlet pairing ψ and triplet pairing d_z and subsequently on the correlation functions F_{-+} and F_{+-}. We showed that for the magnetization of a ferromagnet parallel to the direction of the z-axis (perpendicular to the layers of the two-dimensional systems), which in our model plays a role in the direction of polarization of electrons in the superconductor by SOC interaction, the bound states are formed by the electrons with opposite momentum and spin.

We see a future possibility for development of the work in the analysis of the problem in the case of general orientation of the spin quantization axis which results due to different magnetization orientation of ferromagnetic layer. In such a case the electron pairing is possible not only with opposite spins but also with the same spin orientation. Subsequently, it would be interesting to study density of states, local electron structure and correlation functions of superconductor. Formation of the Cooper pairs with the same spin orientation can be connected with further study of the so-called Majorana fermions, formed at the edges of the real samples.

Next work also opens up a possibility of in-depth analysis of the theory of Gor'kov pairing

symmetries for electrons, which can lead to a better description of the problem and subsequently provide possibility to propose new models for novel systems. A deeper study of the theoretical aspects of condensed matter physics and superconductivity, and quantum field theory is certainly a challenge from personal point of view.

Bibliography

[1] K. S. Novoselov et al. “Electric Field Effect in Atomically Thin Carbon Films”. In: *Science* 306 (2004), pp. 666–669. DOI: 10.1126/science.1102896.

[2] A. H. Castro Neto et al. “The electronic properties of graphene”. In: *Reviews of Modern Physics* 81 (2009), pp. 109–162. DOI: 10.1103/RevModPhys.81.109.

[3] Yuan Liu et al. “Van der Waals heterostructures and devices”. In: *Nature Reviews Materials* 1 (2016), pp. 1–17. DOI: 10.1038/natrevmats.2016.42.

[4] S. Carr et al. “Twistronics: Manipulating the electronic properties of two-dimensional layered structures through their twist angle”. In: *Physical Review B* 95 (2017), p. 075420. DOI: 10.1103/PhysRevB.95.075420.

[5] A. Geim and I. Grigorieva. “Andreev reflection in N/S and F/S junctions”. In: *Nature* 499 (2013), pp. 419–425. DOI: https://doi.org/10.1038/nature12385.

[6] B. T. Zhou et al. “Ising superconductivity and Majorana fermions in transition-metal dichalcogenides”. In: *Phys. Rev. B* 93 (2016), p. 180501. DOI: 10.1103/PhysRevB.93.180501.

[7] Xue Liu et al. “High Performance Field-Effect Transistor Based on Multilayer Tungsten Disulfide”. In: *ACS Nano* 8.10 (2014), pp. 10396–10402. DOI: 10.1021/nn505253p.

[8] Wikipedia the free encyclopedia. *TMD structure*. URL: https://en.wikipedia.org/wiki/Transition_metal_dichalcogenide_monolayers.

[9] N. F. Q. Yuan et al. “Ising Superconductivity in Transition Metal Dichalcogenides”. In: *AAPPS Bulletin* 26 (2016), pp. 12–19.

[10] M. J. Lu et al. “Evidence for two-dimensional Ising, superconductivity in gated MoS2”. In: *Science* 350 (2015), pp. 1353–1357. DOI: 10.1126/science.aab2277.

[11] X. Xi et al. “Ising pairing in superconducting $NbSe_2$ atomic layers”. In: *Nature Physics* 12 (2016), pp. 139–143. DOI: 10.1038/nphys3538.

[12] S. Hunklinger. *Festkörperphysik*. Oldenbourg Wissenschaftsverlag, 2011. Chap. 12.

[13] A. Tirpák. *Elektormagnetizmus*. 1st ed. 1999. ISBN: 80-88780-26-8.

[14] B. Huang et al. "Layer-dependent ferromagnetism in a van der Waals crystal down to the monolayer limit". In: *Nature* 546 (2017), pp. 270–273. DOI: 10.1038/nature22391.

[15] K. Fossheim and A. Sudboe. *Superconductivity: Physics and Applications*. John Wiley & Sons Ltd, 2004. ISBN: ISBN 0-470-84452-3.

[16] J. Bardeen, L. N. Cooper, and J. R. Schrieffer. "Microscopic Theory of Superconductivity". In: *Phys. Rev.* 106 (1957), pp. 162–164. DOI: 10.1103/PhysRev.106.162.

[17] J. Bardeen, L. N. Cooper, and J. R. Schrieffer. "Theory of Superconductivity". In: *Phys. Rev.* 108 (1957), pp. 1175–1204. DOI: 10.1103/PhysRev.108.1175.

[18] A. Costa. "Andreev reflection in N/S and F/S junctions". In: (2014).

[19] F. Schwabl. *Quantenmechanik für Fortgeschrittene*. Springer, 2005. Chap. 1.

[20] C. L. Marvin and S. G. Louie. *Fundamentals of Condensed Matter Physics*. Cambridge University Press, 2016. ISBN: 978-0-521-51331-9.

[21] H. A. Bethe and J. Goldstone. "Effect of a repulsive core in the theory of complex nuclei". In: *Proc. Roy. Soc. (London)* 238 (1957), pp. 551–567. DOI: 10.1098/rspa.1957.0017.

[22] J. S. Galsin. *Solid State Physics: An Introduction to Theory*. Academic Press, 2019.

[23] Wikipedia the free encyclopedia. *Spin–orbit interaction*. URL: https://en.wikipedia.org/wiki/Transition_metal_dichalcogenide_monolayers.

[24] R. Winkler. *Spin-orbit Coupling Effects in Two-Dimensional Electron and Hole Systems*. Springer-Verlag Berlin Heidelberg, 2003. ISBN: 978-3-540-01187-3.

[25] R. J. Elliott. "Theory of the Effect of Spin-Orbit Coupling on Magnetic Resonance in Some Semiconductors". In: *Physical Review* 96 (1954), pp. 266–279. DOI: 10.1103/PhysRev.96.266.

[26] R. J. Elliott. "Theory of the Effect of Spin-Orbit Coupling on Magnetic Resonance in Some Semiconductors". In: *Phys. Rev.* 96 (1954), pp. 266–279. DOI: 10.1103/PhysRev.96.266.

[27] H. A. Kramers. "Théorie générale de la rotation paramagnétique dans les cristaux". In: 33 (1930), pp. 959–972.

[28] I. Zutić, J. Fabian, and S. Das Sarma. "Spintronics: Fundamentals and applications". In: *Rev. Mod. Phys.* 76 (2004), pp. 323–410. DOI: 10.1103/RevModPhys.76.323.

[29] J. Fabian et al. "Semiconductor spintronics". In: *Acta Physica Slovaca* 57 (2007). DOI: 10.2478/v10155-010-0086-8.

[30] A. Kormányos et al. "k.p theory for two-dimensional transition metal dichalcogenide semiconductors". In: *2D Materials* 2 (2015), p. 022001. DOI: 10.1088/2053-1583/2/2/022001.

[31] J.-X. Zhu. *Bogoliubov-de Gennes Method and Its Applications*. Springer International Publishing, 2016. ISBN: 978-3-319-31312-2.

[32] A. S. Alexandrov. *Theory of Superconductivity: From Weak to Strong Coupling*. Institute of Physics Publishing, Bristol and Philadelphia, 2003. ISBN: 978-0750308366.

[33] N. F. Q. Yuan, K. F. Mak, and K. T. Law. "Possible Topological Superconducting Phases of MoS_2". In: *Phys. Rev. Lett.* 113 (2014), p. 097001. DOI: 10.1103/PhysRevLett.113.097001.

[34] L. P. Gor'kov and E. I. Rashba. "Superconducting 2D System with Lifted Spin Degeneracy: Mixed Singlet-Triplet State". In: *Phys. Rev. Lett.* 87 (2001), p. 037004. DOI: 10.1103/PhysRevLett.87.037004.

[35] J. D. Sau et al. "Generic New Platform for Topological Quantum Computation Using Semiconductor Heterostructures". In: *Phys. Rev. Lett.* 104 (2010), p. 040502. DOI: 10.1103/PhysRevLett.104.040502.

[36] M. Sato and S. Fujimoto. "Topological phases of noncentrosymmetric superconductors: Edge states, Majorana fermions, and non-Abelian statistics". In: *Phys. Rev. B* 79 (2009), p. 094504. DOI: 10.1103/PhysRevB.79.094504.

[37] C. Nayak et al. "Non-Abelian anyons and topological quantum computation". In: *Rev. Mod. Phys.* 80 (2008), pp. 1083–1159. DOI: 10.1103/RevModPhys.80.1083.